UNIVERSITY OF CALIFORNIA, MERCED

More Is Better:
Resistant and Susceptible Mouse Model Reveals *Toxoplasma gondii* Glycophosphatidylinositol Anchor to be a Common Natural Antibody Epitope

A thesis submitted in partial satisfaction of the requirements for the degree of Master

of

Quantitative and Systems Biology

by

Jessica Wilson

Committee in charge:
Professor Anna Beaudin, Chair
Professor Juris Grasis
Professor Chris Amemiya
Professor Kirk Jensen, Research Mentor

2019

The thesis of Jessica N. Wilson is approved, and it is acceptable in quality and form for publication on microfilm and electronically:

_____

Dr. Kirk Jensen, Research Mentor

_____

Dr. Juris Grasis

_____

Dr. Anna Beaudin

_____

Dr. Chris Amemiya

University of California, Merced
2019

TABLE OF CONTENTS

Signature Page……..……...……..… 3

List of Figures……....… 6

List of Tables……...…… 7

Abbreviations……...……...……..... 8

Acknowledgement……..……...……...….... 9

Curriculum vitae…….…….... 10 - 13

Abstract…….……...……..... 14

Chapter 1: Introduction

1.1 Toxoplasmosis……...……..15

1.2 Requirements for Immunity to *Toxoplasma gondii*……..…...……..15-16

1.3 Forward Genetic Screen Links *Nfkbid* to Resistance…….16-18

1.4 B-1 Cells……..……18

1.5 Glycophosphatidylinositol Anchors…….……..18-20

1.6 Correlates of Immunity: Defining protective antibody reactivity to the GPI anchor of *T. gondii* ……..…..…….20

Chapter 2: Materials and Methods

2.1 Cells and Medium……21

2.2 Parasite Strains…….21

2.3 Gene Selection for Knock-out of GPI N-Acetylgalactosamine Transferase in *T. gondii*……21-22

2.4 Generation of RHΔ*ku80*Δ*259530::HXGPRT*……..……22-23

2.5 Mice…….……23

2.6 Primary infection and serotyping……...…..……23-24

2.7 Secondary infections and assessment of parasite viability……..24

2.8 Serum Antibody Detection of Parasite Proteins by Western Blotting……..24

2.9 Image Processing and Statistical Analysis of Western Blot Data……25

2.10 Determination of Antibody Dependence and Reactivity to the GPI Moiety in *T. gondii* Lysate Antigen……...….25

2.11 Analysis of *T. gondii* GPI isoform Usage via Flow Cytometry…….26

Chapter 3: Antibodies from chronically infected mice identify GPI-anchored SRS

3.1 Serum antibody reactivity to *T. gondii* lysate antigen is enhanced in resistant compared to susceptible mice……..….…31-33

3.2 B-1 cells may be responsible for a large portion of *T. gondii*-specific antibody: Bumble (*Nfkbid* null) mice generate significantly less antibody to *T. gondii lysate antigen*……..…...34-35

3.3 Hypothesis: A/J and B6 serum antibodies heavily target the GPI anchor of surface antigens……..…36

3.4 Both A/J and B6 serum antibodies require the lipid portion of the GPI anchor for maximal reactivity to *T. gondii* lysate antigen…….37

3.4.1 IgM serum antibody reactivity to antigens below 50kDa requires the GPI lipid moiety…….…..37-39

3.4.2 Total IgG serum antibody reactivity to antigens below 50kDa requires the GPI lipid moiety……...40-42

3.5 Alternative attempts at GPI anchor disruption provide inconclusive results……43-47

3.6 Deleting putative genes encoding the enzyme responsible for generating the side chain of both *T. gondii* glycoforms……..….47-49

3.7 GalNAc Transferase KO: Gene candidate 259530 on Chromosome VIIb……...….49-50

Chapter 4: Discussion

Protective antibody production against the *T. gondii* GPI anchor: More is better……..……..51-52

Conclusion……53

References……..……...……...……... 54-64

LIST OF FIGURES

Figure 1. Disparity in survival outcome to virulent secondary infection

Figure 2. Two GPI glycoforms exist on the surface of *T. gondii*

Figure 3. Infection model

Figure 4. Serum antibody reactivity to *T. gondii* lysate antigen is enhanced in A/J compared to C57BL/6J mice

Figure 5. *Nfkbid* is required for generating *T. gondii*-specific antibody to lysate antigen

Figure 6. A/J and B6 serum IgM relies heavily on the lipid anchor of the GPI structure anchor for detection of *T. gondii* lysate antigen

Figure 7. A/J and B6 serum IgG relies heavily on the lipid anchor of the GPI structure anchor for detection of *T. gondii* lysate antigen

Figure 8. GPI disruption strategy to assess differential binding targets of antibodies from resistant and susceptible mice

Figure 9. HF treatment of lysate on PVDF proves inconclusive due to compromise of internal standard

Figure 10. Jack Bean α-Mannosidase treatment of lysate inconclusive due to overall degradation of sample

Figure 11. *T. gondii* GalNAc transferase gene candidate (259530) KO is not the droid we're looking for

LIST OF TABLES

Table 1. Models and Cell Lines

Table 2. Reagents

Table 3. Equipment

Table 4. Oligos for CRISPR and PCR Design

Table 5. Software and Algorithms

Table 6. Several immunogenic T. gondii proteins below 50kDa are known to be GPI anchored to the outermost parasite membrane

Table 7. Student's t-test of individual western blot bands

Table 8. List of gene candidates scored and ranked for CRISPR targeting of GalNAc adding enzyme

ABBREVIATIONS

Biochemical Groups
GPI: Glycophosphatidylinositol Anchor
Etn: Ethanolamine
Myo-ino: Inositol
PI: phosphoinositol
Lipid Anchor: Alkyl-Glycerol
Gluc: Glucose
GalNAc: N-acetylgalactosamine
Man: Mannose
GlcNAc: N-acetylglucosamine
HF: Hydrofluoric acid
PI-PLC: Phosphatidylinositol-specific phospholipase-C
HEXO: β-N-acetylhexosaminidase
Jack Bean: *C. cannavalis* (Jack Bean) α-Mannosidase

Cytokines
IFNγ: interferon gamma
IL-2: interleukin-2
IL-10: interleukin-10
TGFβ: transforming growth factor beta

Immune cells
CD4: CD4 T cell
CD8: CD8 T cell
B-1: B-1 cell
B-1b: B-1b cell (B-1 cell subset)
B-2: canonical B cell

Immunoglobulins
IgG: immunoglobulin G
IgM: immunoglobulin M

Other terms
FACS: fluorescence-activated cell sorting
IP: intraperitoneal
QTL: quantitative trait loci
TLS: total lane signal
WB: western blot

ACKNOWLEDGEMENT

I am deeply humbled by this experience to have been afforded a small spot on the shoulders of giants. I would like to express my gratitude to the following UC Merced affiliates and outside collaborators:

Dr. Kirk Jensen

Dr. David Gravano

Angel Kongsomboonvech

Scott Souza

Dr. Nicole Baumgarth

Dr. Jean-François Dubremetz

Kristen Valentine

Dr. Ramen Saha

CURRICULUM VITAE

Jessica N. Wilson

Jwilson56@ucmerced.edu * (909) 908-0092

EDUCATION

Master of Science Degree Quantitative and Systems Biology; *GPA: 3.98* *May 2019*
University of California, Merced

Post-Baccalaureate Master's Coursework in Biological Sciences; *GPA: 4.0* *May 2017*
California State University, Fresno

Bachelor of Science Degree in Biological Sciences; Chemistry Minor; *GPA: 3.1* *May 2015*
California State University, Fresno

Associate of Science in Natural Sciences and Mathematics; *GPA: 3.0* *June 2012*
Mt. San Antonio Community College, Walnut

Associate of Arts in Natural Sciences and Mathematics; *GPA: 3.0* *June 2012*
Mt. San Antonio Community College, Walnut

TEACHING EXPERIENCE

University of California, Merced Teaching Assistant **August 2017-Present**

Immunology Lab (BIOL151L) *January 2019-May 2019*
Lectured, demonstrated and guided undergraduates around pipetting skills and techniques, mouse dissection, tissue process, cell count via hemocytometer, flow cytometry, enzyme-linked immunosorbent assay (ELISA), cell culture, western blot, CRISPR/Cas9 design. Students are graded by assessment of a kept lab notebook and formal reports on lab activities written in immunology journal article format.

Immunology Lab (BIOL151L) *August 2018-December 2018*
See above.

Immunology Discussion (BIOL151) *January 2018-May 2018*
Reinforce lecture topics by designing activities that use multiple learning approaches including kinetic, visual and auditory.

Immunology Lab (BIOL151L) *August 2017-December 2017*
See above.

California State University, Fresno Teaching Assistant **Aug. 2015- May 2017**

Biology for Non-Majors Lab *January 2017-May 2017*

Lectured, demonstrated and guided undergraduates around basic animal dissection, microscopy, microscopic sample preparation, comparative anatomy in the context of evolution. Topics span examples from the three Kingdoms as classified by Cavalier-Smith, *et al* 1998 and heavily focuses on Animalia.

Biology for Non-Majors Lab *August 2016-December 2016*

See above.

Biology for Majors Lab *January 2016-May 2016*

Lectured, demonstrated and guided undergraduates around basic animal dissection, microscopy, microscopic sample preparation, comparative anatomy in the context of evolution. Topics span examples from the seven Kingdoms as classified by Cavalier-Smith, *et al* 1998 and heavily focuses on Plantae and Animalia.

RESEARCH EXPERIENCE

Graduate Student Researcher University of California, Merced **August 2017-Present**

- Laboratory of Kirk Jensen, PhD
- Dissected the extracellular parasite moiety required for immunity to secondary exposure in a resistant and a susceptible murine host model.
- Trained in the culture of host mammalian cells and *Toxoplasma gondii*, flow cytometry, fluorescence activated cell sorting, immunofluorescence microscopy, genetic manipulation of *Toxoplasma* via CRISPR/Cas9, polymerase chain reaction, DNA/protein isolation and quantification, transfection, enzyme-linked immunosorbent assay and western blotting.
- Trained in murine handling and restraint, murine colony management, intraperitoneal injection, euthanasia, minimally invasive blood collection, terminal blood collection, bone marrow and organ tissue collection,
- Proficient in ImageLab, GraphPad Prism, Adobe Illustrator, Adobe Acrobat, Photoshop, Microsoft Word, Microsoft Excel, and Microsoft PowerPoint.

Graduate Student Researcher of Parasite Burden CSU, Fresno **August 2015-May 2017**

- Laboratory of Paul Crosbie, PhD
- Investigated the endoparasitic burden of the endangered San Joaquin Valley Kit Fox.
- Trained in collection of digestive tract tissues, tissue storage and process, helminth collection from digestive tract samples, morphological identification of helminths and platyhelminths, helminth preservation, kit tests for *Cryptosporidium* exposure, sanitation control.
- Train undergraduates in the above techniques.
- Proficient in Microsoft Word, Microsoft Excel, and Microsoft PowerPoint.

Undergraduate Researcher of Parasite Burden CSU, Fresno **April 2014-August 2015**

- Laboratory of Paul Crosbie, PhD
- Investigated the endoparasitic burden of the endangered San Joaquin Valley Kit Fox.
- Trained in collection of digestive tract tissues, tissue storage and process, helminth collection from digestive tract samples, morphological identification of helminths and platyhelminths, helminth preservation, kit tests for *Cryptosporidium* exposure, sanitation control.

- Proficient in Microsoft Word, Microsoft Excel, and Microsoft PowerPoint.

Undergraduate Researcher of Cancer Metabolism CSU, Fresno October 2012-April 2014

- Laboratory of Laurent Dejean, PhD
- Investigated the consequences of the over expression of specific Bcl-2 Family proteins on glycolysis, oxidative phosphorylation and lactate dehydrogenase production.
- Trained in mammalian cell culture, cell counts, growth curve assay, classic enzymatic assay, ELISA collaboration, western blot assistance to supervising graduate student, general laboratory housekeeping.

ORAL PRESENTATIONS

Central California Research Symposium Spring 2017

Endoparasite Burden of the Endangered San Joaquin Valley Kit Fox
Awarded Best Graduate Oral Presentation; $250 Cash Prize

POSTER PRESENTATIONS

Central California Research Symposium Spring 2014

Bcl-2 Family protein over-expression differentially effects glycolysis, oxidative phosphorylation and lactate dehydrogenase production.

California State University Program for Education and Research in Biotechnology Spring 2013

See above.

Central California Research Symposium Spring 2013

See above.

AWARDS & SCHOLARSHIPS

Recruitment Fellowship Fall 2017

$5,000 stipend awarded for acceptance to University of California, Merced's Quantitative and Systems Biology Graduate Program.

Phi Kappa Phi Honors Society Spring 2017

Awarded for academic excellence at California State University, Fresno. 4.0 grade point average for four consecutive semesters.

Best Graduate Oral Presentation Spring2017

Central California Research Symposium
$250 Cash Prize

President's Award for Volunteer Service Fall 2012

$2,500 grant awarded for 2,000 hours of outstanding service to the community. Community service project served military veterans and children with special needs through equine therapy.

CERTIFICATIONS

Controlled Substances Handling License — February 2017

Laboratory Safety Training — August 24, 2017
Lab Safety Fundamentals with Hazmat Spill Response

Laboratory Safety Training — August 25, 2017
Biosafety with Bloodborne Pathogens and Air Transmissible Disease

Laboratory Safety Training — September 11, 2018
Fire Safety

ABSTRACT

More Is Better:
Resistant and Susceptible Mouse Model Reveals *Toxoplasma gondii* Glycophosphatidylinositol Anchor to be a Common Natural Antibody Epitope

By

Jessica N. Wilson

Master of Science in Quantitative and Systems Biology

University of California, Merced 2019

Professor Anna Beaudin, Chair

Parasitic disease is a global health burden. Current and historical efforts to eradicate parasitic disease rely heavily on vector control and mass drug administration campaigns rather than vaccine induced immunity due in large part to effective parasite immune evasion. *Toxoplasma gondii* is an intracellular protozoal parasite estimated to infect up to a third of the world's population, is the second leading cause of food-borne disease in the United States and demonstrates evasion of vaccine induced immunity (CDC, 2017). Previous work done by our lab suggest a crucial role for B-1 cells for the control and clearance of highly virulent *T. gondii* strains. A genetic link between *Nfkbid* and the resistant murine phenotype prompted our endeavor to analyze antibody reactivity to *T. gondii*. We used serum antibody to probe *T. gondii* protein via western blot and found 1) A/J and C57BL/6J serum IgM and total IgG antibody target the same proteins below 50kDa which are likely known GPI anchored proteins, 2) B-1 cell deficient *Nfkbid* null C57BL/6J mice lose 87% serum IgM reactivity and 91% total IgG reactivity when compared to wild type C57BL/6J mice, 3) A/J and C57BL/6J antibody reactivity to *T. gondii* protein relies heavily on the presence of the lipid moiety of the GPI anchor and 4) A/J mice to produce more antibody overall than C57BL/6J mice. These findings contribute to our growing body of work which correlates resistance to *T. gondii* infection with enhanced antibody production to antigens likely targeted by B-1 cells. Resolution of the contribution of this protective antibody response may provide novel insight for the development of a completely protective and long-lasting vaccine against parasite.

CHAPTER 1

1. Introduction

1.1 Toxoplasmosis

Toxoplasma gondii is a ubiquitous intracellular parasite of warm blooded animals that is estimated to infect up to one third of the global human population (CDC, 2017). As the second leading cause of death by food borne illness in the United States (CDC, 2017), toxoplasmosis and other parasitic disease on the whole is of medical importance responsible for 96 million disease-adjusted life years (DALYs) and 1 million deaths worldwide (Cundill et al., 2011; Hotez et al., 2014; Pullan et al., 2014; Torgerson et al., 2014, 2015). Although toxoplasmosis in healthy individuals is generally asymptomatic, chronic carriers who become immunocompromised can develop toxoplasmic encephalitis as a result of tissue cyst rupture and reactivation of dormant parasites (Luft et al., 1993). Acquisition of *T. gondii* during pregnancy is potentially dangerous for the unborn child because *T. gondii* can cross the placenta (Kieffer and Wallon, 2013). As the causative agent of congenital toxoplasmosis (CT), *T. gondii* infection in utero can manifest as chorioretinitis, intracranial calcifications and hydrocephaly, if the child survives (Lindsay and Dubey, 2011; McAuley, 1994; Swisher et al., 1994). Despite this global health burden, the development of a protective vaccine for humans against *T. gondii* and other protozoal pathogens has been elusive (Sacks, 2014). *T. gondii* is a member of the phylum Apicomplexa and shares many of the characteristics of *Plasmodium* spp., the causative agent of malaria, including replication within a parasitophorous vacuole and use of secretory products from apical organelles to modulate host cells (Chakraborty et al., 2017). Immune evasion mechanisms employed by these parasites make them difficult targets for treatment and vaccine development. Even when hosts are chronic carriers, or at least have had previous exposure, protection conferred by immunological memory can be incomplete against other *T. gondii* strains (Jensen et al., 2015) and is not completely preventative of congenital toxoplasmosis (Elbez-Rubinstein et al., 2009). Currently, there is only one vaccine against a human parasitic disease, malaria, with an underwhelming efficacy of 27% (RTS,S/AS01) (RTS Clincal Trials Partnership, 2015). Vaccine design in general often fails to elicit long-lasting T cell effector responses required for the clearance of parasitic pathogens (Sacks, 2014; Sher, 1992). The understanding of the requirements for long-lasting immunity to parasite is crucial for continued aim of completely protective vaccine development.

1.2 Requirements for immunity to *Toxoplasma gondii*

Toxoplasma immunologists have long made a case for the critical role of CD8 T cells and IFNγ for the control and clearance of parasitic infection (Shirahata et al., 1994; Y Suzuki,

MA Orellana, RD Schreiber, 1988; Y Suzuki, 1989). Although a variety of immune cells play a role in fighting an initial infection (i.e. 'primary infection') (Yarovinsky, 2014), in cases where mice were either chronically infected or vaccinated with replication deficient (avirulent) strains of *T. gondii*, CD8 T cells were found primarily responsible for protection against lethal secondary infection (or 'challenge') with the highly passaged Type I RH strain (lethal dose of one parasite in naïve mice) (Gazzinelli et al., 1991; Gigley et al., 2009, 2011; Nagasawa et al., 2013; Suzuki and Remington, 1988). For example, adoptively transferred memory CD8 T cells can confer immunity in naïve mice to many strains of *T. gondii* that would otherwise cause lethal infection (Buzoni-Gatel et al., 1997; Gigley et al., 2009; Suzuki and Remington, 1990) and IFNγ responses are necessary in this setting (Gigley et al., 2009; Suzuki and Remington, 1990). In contrast, CD4 T cells which generate copious amounts of IFNγ during secondary infection (Splitt et al., 2018), when depleted or adoptively transferred, do not reduce or confer protection to *T. gondii* challenge, respectively (Gigley, Fox, and Bzik 2009; Gazzinelli et al. 1991; Jordan et al. 2009). However, not all strains of *T. gondii* are controlled by immunological memory responses conferred by vaccination or chronic infection (Jensen et al., 2015) and most virulent strains, including the Type I RH strain, are refractory to IFNγ-induced killing mechanisms (Niedelman et al., 2012) suggesting additional immune mechanisms must exist to control virulent strains of *T. gondii*. Consistent with this supposition, virulent *T. gondii* strains, including the Type I RH strain, encode an arsenal of virulence factors that resist IFNγ-elicited killing mechanisms including rhoptry proteins ROP5, ROP18, ROP17 and TgIST, which act to block IFNγ-induced immunity-related GTPases (IRGs) that destroy the parasitophorous vacuole necessary of intracellular life (Howard et al., 2011) and IFNγ-induced STAT1 activation in the host cell (Gay et al., 2016; Olias et al., 2016), respectively. Yet, immunological memory is possible against the Type I RH strain. What additional cell-mediated mechanisms are required for immunity are currently unknown but cytotoxicity conferred by perforin and NO production are dispensable (Khan et al., 1997). Discovery of new modes of immunity to virulent strains of *T. gondii* is an overarching goal of this dissertation.

1.3 Forward genetic screen links *Nfkbid* to resistance

In previous work, our lab has demonstrated a disparity in survival to secondary infection with the highly virulent Type I GT1 *T. gondii* strain in A/J and C57BL/6J ('B6') mice (Souza, S., Splitt, S., unpublished) (Figure 1). Since the genetic background of a host is implicated in the outcome of infection with *T. gondii* (Sher, 1992), a forward genetic screen of 26 recombinant inbred mice, derived from crossing A/J and C57BL/6 mice, was performed and provided valuable clues to the specific genetic differences which afford resistance or susceptibility to secondary infection. The 26 recombinant inbred mice (AxB;BxA) have an assortment of homozygous A/J and B6 alleles and allow for genetic mapping of loci that contribute to host variation in survival and transcriptional responses to *T. gondii* infection (Hassan et al., 2014, 2015; McLeod et al., 1989). Genetic mapping for host resistance to secondary infection revealed two distinct Quantitative Trait Loci (QTL) peaks with logarithm of the odds (LOD) scores greater than three on chromosomes 7 (LOD = 3.57, imputed marker between rs8261820 and rs8261944) and 10 (LOD = 3.29,

imputed marker between rs13480776 and rs13480777) (Splitt, S. unpublished). Although neither of these peaks reached significance upon permutation testing (n = 100; $p<0.05$, LOD = 5.5), previous endeavors by other labs have shown non-significance should not necessarily invalidate further investigation; as occurred for the successful identification of MHC 1 L^d as the host resistance factor to chronic *T. gondii* infection via QTL analysis (Brown et al., 1995; McLeod et al., 1989).

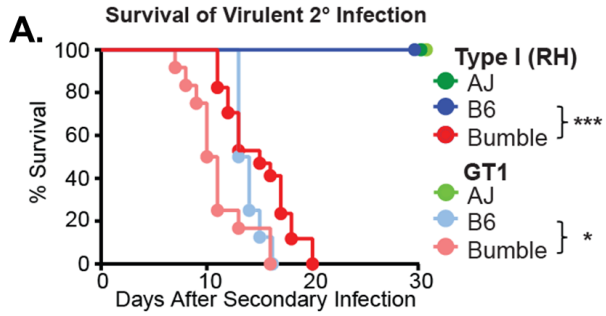

B.

T. gondii Strain	Primary Infection		Challenge	
	AJ$^{\alpha}$	B6$^{\alpha}$	AJ$^{\beta}$	B6$^{\kappa}$
CEP	100	100	100	100
RH	0	0	100	100
GT1	0	0	100	0

Figure 1. Disparity in survival outcome to virulent secondary infection. A. *Survival of virulent secondary infection is differential among A/J, B6 and Bumble mice: A/J is fully resistant to the challenge where B6 survival is contingent on the parasite strain. Bumble (Nfkbid null, C57BL/6 background) succumb to secondary challenge with RH and 3-5 days sooner than B6 with GT1 challenge. Log Rank Mantel-Cox significance *P<0.05; ***P<0.0001 (Souza, S. unpublished).* ***B.*** *Table of survival outcomes of A/J and B6 mice primed or challenged with CEP, RH or GT1 T. gondii strains (Ref. α Sibley 1992, β Souza, S. unpublished, κ Jensen, et al. 2015).*

Closer inspection of the QTL on chromosome 7 revealed a highly polymorphic gene *Nfkbid* closest to the rs8261820 and rs8261944 markers, also known as IκBNS (Splitt, S. unpublished). IκBNS is a member of the atypical NF-κB inhibitors, is restricted to the nucleus and known to modulate NF-κB to induce or repress transcription (Schuster et al., 2013). IκBNS functionality has been found to enhance T cell production of IL-2 and IFNγ (Clayton et al., 2007), T and B cell expression of IL-10 (Miura et al., 2016), support development of T regulatory cells (Schuster et al., 2012) and suppresses Toll-like receptor (TLR)-induced cytokine expression in macrophages (Hirotani et al., 2005, 2006). Importantly, in the absence of IκBNS, the most extreme phenotype observed is mouse B-1 cell development and functional absence (Arnold et al., 2012; Pedersen et al., 2016; Touma et al., 2011). This results in the hosts' inability to respond to T-independent type II antigens, like (4-hydroxy-3-nitrophenyl)-acetyl (NP)-Ficoll, and generate circulating IgM and IgG3 antibodies (Pedersen et al., 2016).

We therefore screened the role of *Nfkbid* null mice (bumble) in their ability to generate immunity to virulent secondary *T. gondii* infections and determined these mice were highly susceptible (Figure 1A) (Scott, S unpublished). Moreover, *Nfkbid* null mice were unable to generate any parasite-specific IgM and had greatly diminished parasite-specific IgG responses of all isotypes (not shown) and had defects in generated neutralizing serum

antibodies following infection (Souza, S unpublished). We believe this is a critical clue in deciphering the requirements for resistance to secondary *T. gondii* infection and that IκBNS-dependent B cell responses to T-independent antigens may be a central feature of immunity to this parasite.

1.4 B-1 cells

B cell response is a crucial component of humoral immunity that results in protective antibody against future re-exposure to pathogen and is the foundation of vaccine design. B cells are now known to exist as two distinct lineages, numerically labelled based on their sequential appearance in ontogeny: the canonical B-2 and the primordial B-1 (Baumgarth, 2011; Berland and Wortis, 2002). In adults, B-2 cells differentiate from hematopoietic precursors found in the bone marrow and are known to produce antibody against protein antigen. In contrast, B-1 cells are a self-renewing population of B cells that are highly enriched in the peritoneal and pleural cavities of mammals and generate non-redundant antibody responses that focus against self- and/or non-protein antigens (Baumgarth, 2011, 2016; Baumgarth et al., 2000a; Berland and Wortis, 2002). B-1 cells secrete 'natural antibodies' in the absence of infection and can bind oxidized lipids (Chou et al., 2009), phosphatidyl choline and annexin V of apoptotic cells (Kulik et al., 2009), and the GPI-anchored protein Thy-1 (Hayakawa et al., 1999). Moreover, B-1 cells have been found by various researchers to be responsible for specific pathogen-induced immune responses in studies of immunity involving the following pathogens: *Francisella* spp (Cole et al., 2009; Yang et al., 2012), *Borrelia hermsii* (Alugupalli et al., 2003, 2004; Colombo and Alugupalli, 2008), *Salmonella typhi* (Cunningham et al., 2014; Gil-Cruz et al., 2009), *Streptococcus pneumoniae* (Briles et al., 1981; Cosenza and Kohler, 1972; Haas et al., 2005), and influenza virus (Baumgarth et al., 1999, 2000b; Choi and Baumgarth, 2008)—most of which are intracellular pathogens (Baumgarth, 2016). Two distinct B-1 cell subsets have been defined as B-1a and B-1b primarily by the presence of CD5, respectively (Baumgarth, 2016). Although theories around the individual roles of B-1a and B-1b that comprise B-1 cells remain to be fully resolved, both natural and pathogen-elicited IgM is a clearly critical means of pathogen resistance (Smith and Baumgarth, 2019).

1.5 Glycophosphatidylinositol Anchors

The surface of *T. gondii* is known to be dominated by proteins linked by glycophosphatidylinositol (GPI) anchors (Manger et al., 1998; Nagel and Boothroyd, 1989). GPI anchors are conserved across the animal kingdom and, although have differences in side chain additions, are otherwise structurally conserved as well (Ferguson, 1999; Fontaine et al., 2003; Homans et al., 1988; Low, 1987; Naik et al., 2000; Nosjean, O., Briolay, A., and Roux, 1997; Paulick and Bertozzi, 2008). In *T. gondii* and other species, the core structure is defined by α-Man-(1→2)- α -Man-(1→6)- α -Man-(1→ 4)- α -GlcNAc-(1→6)-myo-Inositol-PO_4-lipid (Ferguson, 1999)(Figure 1). *T. gondii* has been found to express six GPI anchor isoforms each different combinations of the side chain or ethanolamine attached to the core structure (Striepen et al., 1997) but there are only two

glycoforms that differ in their sugar composition (Striepen et al., 1997; Zinecker et al., 2001). These two GPI glycoforms are distinguished by a side chain addition of β-GalNAc to the mannose with or without a terminal glucose, α -Glc-(1→4)-β-GalNAc (Striepen et al. 1997) (Figure 2). Although much of the initial work done to characterize this assembly was done in trypanosomes, *T. gondii* construction of the GPI occurs in multiple identical stages in the ER where the synthesis of the precursor starts with the transfer of GlcNAc to phosohoinositol (PI) from UDP-GlcNAc, and following de-N-acetylation, resulting in GlcN-PI (Bangs et al., 1988; Englund, 1993). Dol-P-Man is used as donor for the subsequent mannosylation (Menon et al., 1990; Tomavo et al., 1992a) and synthesis is

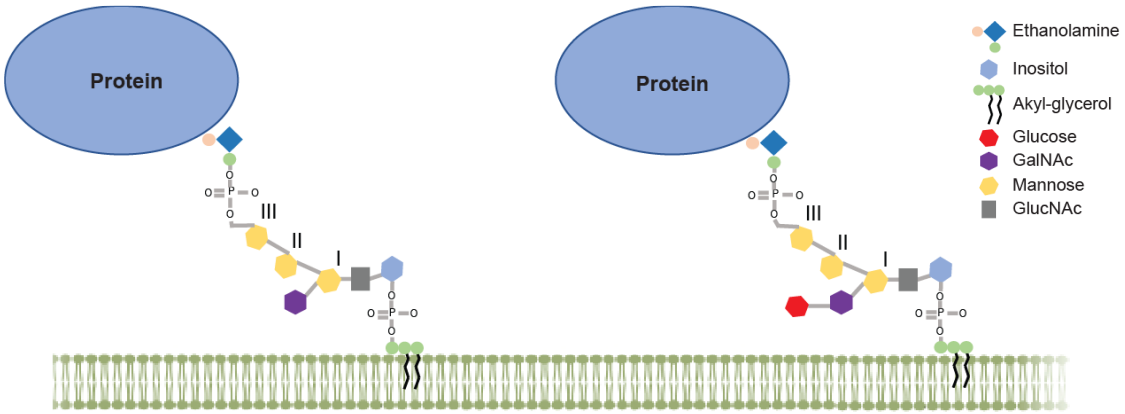

Figure 2. Two GPI glycoforms exist on the surface of T. gondii. *T. gondii has 6 isoforms but only two glycoforms. Both glycoforms share the same core structure: (top down) if attached, the protein binds an ethanolamine group at its N-terminus. The ethanolamine group is bound to a phosphate group which is bound to a three-mannose core backbone structure. The mannose backbone is bound to a N-acetylglucosamine (GlucNAc), inositol, phosphate group and finally the lipid anchor (alkyl-glycerol) imbedded into the hydrophobic span of the outer membrane. Where the glycoforms differ is the side chain off of the first mannose group: one glycoform has a terminal N-acetylgalactosamine (GalNAc) while the other has a glucose added to the GalNAc (Striepen, et al. 1997). Both glycoforms are expressed simultaneously and, between specific strains, are differentially expressed (Niehus, S. et al. 2014). Both glyco-forms are expressed with and without protein addition to the ethanolamine group. The other GPI isoforms differ in acyl tail composition and some lack the ethanolamine group when not attached to a protein (Striepen, et al. 1997).*

completed by transfer of ethanolamine phosphate from phosphatidyl-ethanolamine (Menon et al., 1993). Side chain additions occur on the cytoplasmic face of the ER (Smith et al., 2006). The most immunogenic portions of the *T. gondii* anchor in humans are thought to be the glucose addition to the β-GalNAc side chain (Gçtze et al., 2014; Seeberger et al., 2011; Striepen et al., 1997). GPI anchors have been shown to play a role in the stimulation of MMP-9 which functions to degrade cellular structures of macrophage in mice (Guérardel et al., 2011) and activate NF-kB through TLR4 (Debierre-Grockiego et al., 2007), contributing to immune response and invasion. Vaccination with synthesized GPI

anchors conjugated to non-toxic diphtheria toxin mutant CRM197 have been shown to elicit antibody responses to the anchor but fail to provide complete protection from live parasite (Götze et al., 2015). Additionally, vaccination with parasite proteins or DNA constructs encoded with single *T. gondii* proteins alone also fails to provide complete protection (Hoseinian Khosroshahi et al., 2011; Ismael et al., 2003; Pinzan et al., 2015). Taken together, we find there is novel opportunity to pursue a long-lasting vaccine design that incorporates protein antigen to generate T cell response as well as T-independent antigens, such as the GPI anchor, to elicit a crucial B-1 cell response to provide comprehensive protection against live *T. gondii* parasite.

1.6 Correlates of Immunity: Defining protective antibody reactivity to the GPI anchor of *T. gondii*

A substantial amount of work has been done to resolve requirements for immunity to *T. gondii* and identify antigenic targets applicable for vaccine design. Although classical serum antibody analysis has been done using human and mouse serum to identify major antigens on the surface of *T. gondii*, a genetically disparate host infection model has never been used to decipher antibody targets and whether such targets differ between genetically resistant and susceptible hosts. In chapter 3, sections 1 through 3, I utilize serum antibody from resistant and susceptible murine hosts to estimate differential IgM and total IgG antibody production against *T. gondii* whole parasite lysate antigen separated via SDS-PAGE. I found that this not only recapitulated previous works of heavily targeted antigens below 50kDa but found that genetically resistant mice produce more parasite-specific IgG and IgM antibody (but only in the challenge condition) to *T. gondii* lysate antigen following infection. In sections 4 and 5, I dismantle the GPI anchor by enzymatically removing key immunogenic portions of the anchor and demonstrate that antibody reactivity to *T. gondii* is highly dependent on an intact GPI anchor of the 50kDa-20kDa antigens, consistent with previously described surface protein antigens of *T. gondii* (i.e. 'SAG' or 'SRS' proteins) with corresponding molecular weight ranges. These observations suggest that targeting of non-protein moieties of the SAGs GPIs are likely instrumental for immunity to *T. gondii*, particularly during secondary infection. In sections 6 and 7, I strategize to remove the putative immunogenic component of the GPI anchor: the α-Glc-(1→4)-β-GalNAc side chain. Because the enzyme that is responsible for adding β-GalNAc to (the first) mannose during *T. gondii* GPI assembly is currently unidentified, a list of gene candidates has been compiled which offer a ranked list of targets for removal. Using CRISPR deletion techniques, I disrupted one of the selected gene candidates and cloned edited parasites with the intention of confirming the loss of β-GalNAc via flow cytometry and infecting primed resistant mice. We hypothesize primed resistant mice would succumb to secondary infection in the absence of the side chain epitope for protective antibody recognition. The correct identification of this enzyme would afford conclusive evidence that the side chains generated by *T. gondii* are required for protective antibody recognition of parasite.

CHAPTER 2

Materials and Methods

2.1 Cells and Medium

Human foreskin fibroblasts (HFFs) monolayers were grown at 37°C, 5% CO_2 in T-25 flasks for parasite passaging in 'HFF medium' (Dulbecco's modified Eagle's medium [DMEM; Life Technologies] supplemented with 2mM L-glutamine, 20% fetal bovine serum [FBS; Omega Scientific], 1% penicillin/streptomycin cocktail [Life Technologies], and 0.2% gentamycin [Life Technologies]. T-25 flasks were made by splitting T-175 flasks 1:50. T-175 flasks were washed with 20mL sterile PBS and 3mL trypsin was added. Flasks were incubated for 10 minutes at 37°C, 5% CO_2. Monolayers were agitated by tapping the flask and 200 mL HFF medium was added; 4mL of cell suspension was placed in each T-25 flask. T-25 flasks were ready for passaging after 1-2 weeks.

2.2 Parasite Strains

Toxoplasma gondii strains were serially cultured in HFF (human foreskin fibroblasts) at 37°C, 5% CO_2 in T-25 flasks with 1X Dulbecco's Modified Eagle Medium [(DMEM)+GlutaMAX^{TM}-1 with 4.5g/L D-Glucose, Life Technologies], supplemented with 1% heat-inactivated FBS and 1% penicillin/streptomycin cocktail [Life Technologies]. The following clonal strains were used (clonal types are indicated in parentheses): RHΔ*ku80*Δ*hxgprt* (type I), RHΔ*ku80*Δ*259530::HXGPRT* (type I), RH1-1 (type I), GT1 (type I), and CEP (type III).

2.3 Gene Selection for Knock-out of GPI N-Acetylgalactosamine Transferase in *T. gondii*

The enzyme which adds the terminal glucose and/or terminal N-acetylgalactosamine to the *T. gondii* GPI isoform has not been identified. Recently, an enzyme that performs this function was found in humans: PGAP4 (Gene symbol: *TMEM246; Protein: Q9BRR3|TM246_HUMAN*). Specific characteristics of this enzyme include three transmembrane domains and a catalytic site with the amino acid sequence, EDD, where it catalyzes the addition of N-acetylgalactosamine to the first mannose in the GPI backbone (Hirata et al., 2018). We thought to utilize this discovery to narrow the list of possible candidates in the *T. gondii* genome. To do so, we employed a strategy to find the putative B1–4GalNAc GPI transferase, as the human gene of PGAP4 has no clear homolog in the *T. gondii* genome (Hirata et al., 2018).

First in the *T. gondii* database, ToxoDB.org (Release 41, January 2019), a text search of gene names, gene notes and/or description was performed using the comprehensively annotated Me49 genome for the terms or words containing "GalnAc transferase*",

"glycosyltransferase*", "nucleotide-diphospho-sugar transferases*", "galactosyltransferase*", OR "n-acetylgalactos*" (*wildcard designates the text can be embedded within a word); this generated a list of 225 genes. Because the GPI synthesis pathway occurs mainly in the ER using enzymes with transmembrane domains (Eisenhaber et al., 2018), including PGAP4 (Hirata et al., 2018), we reasoned the putative B1–4GalNAc transferase must contain at least one predicted transmembrane domain; this portion of the search was done looking for predicted transmembrane domains for a gene's homolog in all sarcocysts; this reduced the list to 54 genes. Furthermore, given PGAP4 uses an EDD in its catalytic site (Hirata et al., 2018), and most gylcosyl-transferases use a DxD motif to transfer dinucleotide-sugars (Albesa-Jove and Guerin, 2016; Wiggins and Munro, 1998), the list was further refined to include only those with either EDD or DxD motifs producing 37 genes. The unidentified *T. gondii* B1–4GalNAc GPI transferase uses the nucleotide sugar UDP-GalNAc to transfer this sugar to the first mannose of the GPI backbone (Smith et al., 2007).

Finally, candidates performing irrelevant biologies (e.g. rTRNA synthases, zinc fingers, etc.) or known members of the core GPI synthesis pathway (e.g. PIG-M, etc.), were removed from this list producing a total of 11 candidates.

Scoring for Gene Target Selection: For remaining criteria, the candidates were given binomial scores where the sum of those scores provided a rank order list of candidates: a) Expression; ≥5FPKM is indicative detectable expression in tachyzoites ≥5 score 1. b) EDD; the characterized amino acid sequence of the catalytic domain of PGAP4, EDD score 1. c)Signal peptide; places the protein product in the secretory pathway and/or ER integration Signal peptide score 1. d) "Biologically correct"; a gene possesses characteristics predictive of a sugar transferase transferase is given a score of one. e) rTRNA synthases; GPI synthesis enzymes and irrelevant products are given a score of 0. The results of this strategy are displayed in Table 8.

The human PGAP4 amino acid sequence was blasted (BLASTP) against the Me49 protein database and returned a single gene (255240) with a poor score and high E-value (E=1.5). The gene has an EED sequence but lacks a transmembrane domain and signal peptide. Its function is uncharacterized but has a non-SMC mitotic condensation complex subunit 1 domain, giving a 0 for the "Biologically correct" category. This gene is added to Table 8 for comparison.

2.4 Generation of RHΔ*ku80Δ259530::HXGPRT*

CRISPR/Cas9 technique was used to manipulate the homology directed repair restricted RHΔ*ku80* strain. CHOPCHOP (Labun et al., 2016; Montague et al., 2014) designed CRISPR guides (5'-GCTGAGTCCTAGTGCAC, GTGCACTAGGACTCAGC) were chosen to target the first exon locus (259530) on chromosome VIIb of *T. gondii*. RHΔ*ku80* parasite strains were transfected with a plasmid encoding designed CRISPR guides and CAS9 and co-transfected with a drug resistance cassette *HXGPRT* containing homology arms. Homology directed repair of the CAS9 cut site with the drug selectable marker allows drug selection and gene editing at the locus. Transfectants were grown in MPA+xanthine

supplemented selection media. DNA isolation of bulk transfected population was done using DNAzol and probed for desired insertion by PCR with Mango Mix and diagnostic locus specific primers (5'- TTTCTGCATTTCCCTGTCGCTACC, TTGACCCCCCTCGTATCCGAG). Primer designs were synthesized by and purchased from Integrative DNA Technologies (IDT). Alternative gene targets and their respective designed guide RNAs, primers and homology arms are listed in reagents list. Once target editing was confirmed, the transfected bulk population was serially diluted to isolate on-target clones from off-target or unedited parasites. Clonal populations were assessed via PCR using Mango Mix with the aforementioned designed primers as well as primers specific for the selectable marker (listed in Table 4) to determine positive single insertion and orientation.

2.5 Mice

A/J (Stock# 000646) and C57BL/6J (B6) (Stock#000664) inbred mice were purchased from Jackson Laboratories. For all experiments, age matched females were used at 6-8 weeks, 3-5 mice per infection condition.

Bumble mice (C57BL/6 background), which are *Nfkbid* null due to mutation by ENU mutagenesis (Arnold et al., 2012), were generously gifted by Dr. Nicole Baumgarth in collaboration with the University of California, Davis. For all experiments, age matched bumble and C57BL/6 females were used at 6-8 weeks, 3-5 mice per infection condition.

All mice were maintained in the pathogen-free animal facility at the University of California, Merced. All animal experimentation in this study was performed in accordance with the National Institutes of Health *Guide to the Care and Use of Laboratory Animals* and approved by the Institutional Animal Care and Use Committee (IACUC) (AUP17-0013), Animal Welfare Assurance filed with OLAW (#A4561-01), USDA (93-R-0518), and the University of California, Merced accredited Animal Care Program is AAALAC (001318).

2.6 Primary infection and serotyping

Parasite injections were prepared by scraping T-25 flasks containing vacuolated HFFs and sequential syringe lysis first through a 25G needed followed by a 27G needle. The parasites were spun at 400 rpm for 5 minutes and the supernatant was transferred to a new tube, followed by a spin at 1700 rpm for 7 minutes. The parasites were washed with 10mL phosphate-buffered saline (PBS), spun at 1700 rpm for 7 minutes, and resuspended in PBS and counted with a hemocytometer. For chronic infections with CEP, mice were infected intraperitoneally (IP) with 10^4 tachyzoites in 200µL sterile 1X PBS. Parasite viability of the inoculum was determined by plaque assay following IP infections. Briefly, 100 and 300 tachyzoites were plated in HFF monolayers grown in a 24-well plate and 4-7 days later parasite plaques were counted by microscopy (4x objective).

Between 30-35 days following chronic infection, 50 µL of blood was harvested from mice from the tail vein or humanely euthanized via CO_2 inhalation and terminally exsanguinated

from the retro-orbital vein following enucleation. Whole blood was collected in tubes containing 5µL or 10µL 0.5M EDTA and placed on ice. The blood was pelleted at 10,000 rpm for five minutes; serum was collected from the supernatant and stored at -80°C until use. To evaluate seropositivity of the mice, HFFs were grown in 24 well plates and infected with RH1-1 overnight, washed with PBS, fixed with 3% formaldehyde in PBS, washed with PBS, permeabilized with 3% goat serum, 0.2M Triton X-100-0.01% sodium azide, incubated with a 1:100 dilution of collected serum for 2 hours at room temperature or overnight at 4°C, washed with PBS, and detected with Alexa Fluor 594-labeled secondary antibodies (1:1,000) specific for mouse IgG [Life Technologies]. Seropositive parasites were observed by immunofluorescence microscopy.

2.7 Secondary infections and assessment of parasite viability

Seropositive mice were challenged with $5x10^4$ syringe-lysed GT1 parasites injected IP. After five days of challenge, mice were humanely euthanized and terminally exsanguinated for experiments. Collected whole blood samples were centrifuged to separate serum from whole blood as previously articulated and stored at -80°C until use. Parasite viability for each strain was determined by plaque assay following completion of injections.

2.8 Serum Antibody Detection of Parasite Proteins by Western Blotting

To generate parasite lysate antigens for SDS-PAGE separation and analysis, various *Toxoplasma gondii* strains were cultured in HFF (human foreskin fibroblasts) and expanded to approximately $2x10^8$ parasites. Parasites were syringe-lysed, washed with sterile 1X PBS and parasite pellet was solubilized with (1mL) 0.1% TritonX-100 detergent in 1X PBS (Mayor et al., 1990a). Solubilized parasites were centrifuged at 2,000 rcf for 20 minutes at 4°C to remove large debris and supernatant was collected and aliquoted (50µl) for storage at -80°C until use. Enrichment for glycosylated proteins was not done. Protein concentration was measured by Pierce BCA Protein Assay Kit (Thermo Fisher Scientific) according to the manufacturer's protocol.

Lysate was removed from cold storage and thawed on ice. 50µl of thawed lysate was reduced with 12µL β-mercaptoethanol (BME) and (1.04 mg of lysate protein per lane) separated via SDS-PAGE before transfer to PVDF membrane via Transblot Turbo [Biorad]. Membranes were blocked with 10% fortified bovine milk dissolved in 1X Tris-Buffered Saline with 0.1% Tween (TBS-T 0.1%) (block) for 1-2 hours at room temperature or overnight at 4°C. Blots were then probed with heat inactivated serum (30 minutes at 56 °C) in block at either 1:1,000 dilution for serum IgM analysis or 1:5,000 dilution for serum IgG analysis overnight at 4°C. Membranes were washed with approximately 20mL (each) TBS-T 0.1% three times at 10-20 minutes per wash. Blots were then secondarily probed for one hour at room temperature with goat α-mouse horseradish peroxidase (HRP)-conjugated antibodies: anti-IgM secondary 1:1,000 and total anti-IgG secondary 1:5,000 (specific antibodies listed in Table 2). Membranes were then washed approximately 20mL (each) TBS-T 0.1% three times at 10-20 minutes per wash and developed with Immoblion® Forte Western HRP Substrate. All blots were imaged via chemiluminescence on a ChemiDoc Touch [Biorad].

2.9 Image Processing and Statistical Analysis of Western Blot Data

Image Lab software [Biorad] was used for analysis of bands and total lane signal. Image Lab Files from ChemiDoc were imported to Image Lab for analysis and values were exported to Excel for compilation. Specifically, molecular weights of individual bands were calculated by Image Lab and inferred from the molecular marker [BioRad Precision Plus Standard Protein Ladder]. Assigned molecular weights were used as a means for band comparison and consensus across blots from different experiments. The consistency of the serum antibody banding pattern from this model afforded consensus between blots performed at different times by averaging the calculated molecular weight of each band. These averages informed the manual labelling of each band of P22, P30, and so on, as a means of direct comparison of antibody recognized proteins of interest. The borders of each band were defined by hand in Image Lab and subsequent volume intensity values were adjusted for the background signal specific to each blot; these values were exported to excel for organization. To further control for variability between blots, we normalized treatment conditions to control (mock) conditions to assess loss of signal due to treatment within each blot. Similarly, lane and/or band signal obtained from different mouse genetic backgrounds were normalized against each other, as blots using serum from resistant and susceptible mice were always imaged side by side. These values were exported to GraphPad Prism 7 for statistical analysis and graphical representation.

2.10 Determination of Antibody Dependence and Reactivity to the GPI Moiety in *T. gondii* Lysate Antigen

Parasite lysate (see 2.8 for preparation) was thawed on ice prior to enzymatic treatment. Once thawed, 50µL lysate was incubated at 37°C for 1 hour with 0.5 units of Phosphatidylinositol-specific phospholipase C (PI-PLC), isolated from *B. cereus* [Life Technologies], at a V:V ratio of 10:1 (lysate:PI-PLC), respectively, in the presence of a protease inhibitor cocktail [Fisher] used at 1X of reaction volume. Samples were then reduced with 12µL BME in sample loading dye (approximately 0.8mg parasite protein per well) and loaded into Pre-Casted Mini-PROTEAN TGX Gels [Biorad] at a 4-20% SDS gradient.

Again, parasite lysate (see 2.8 for preparation) was thawed on ice prior to enzymatic treatment. Lysate was incubated at 37°C for 1 hour with 0.5-75 units per 1 mg of *T. gondii* lysate of recombinant β-N-acetylhexosaminidase$_f$ [New England Biotechnologies] at a variable V:V ratio, in the presence of a glycobuffer [New England Biotechnologies] used at 1X of reaction volume. Samples were then reduced with BME and loaded into Pre-Casted Mini-PROTEAN TGX Gels [Biorad] at a 4-20% SDS gradient.

Lysate was thawed on ice prior to incubation at room temperature (approximately 21°C) for 12, 24 and 48 hours with 3.6 units of Jack Bean α-Mannosidase, isolated from *Canavalia ensiformis* [Sigma] at a V:V ratio of 10:1 (lysate:enzyme), respectively, in the presence of a protease inhibitor cocktail [Fisher] used at 1X of reaction volume. Samples were then reduced with BME (approximately 0.7mg parasite protein per well) and loaded into Pre-Casted Mini-PROTEAN TGX Gels [Biorad] at a 4-20% SDS gradient.

PVDF membranes with separated lysate was placed in an acidic bath of 48% hydrofluoric acid for 6, 12, 24, 48 and 60 hours at 4°C. Membranes were then removed from HF, bathed in filtered and distilled water, then 1XPBS before subsequent block and probe (as previously described).

2.11 Analysis of *T. gondii* GPI isoform Usage via Flow Cytometry

RHΔ*ku80* (parental) and RHΔ*ku80*Δ*259530::HXGPRT* (knock out) parasite strains were passaged in HFF with 'Toxo media,' as previously articulated. On the day of analysis, parasites were syringe lysed, pelleted, washed with 1X PBS and counted with a hemocytometer. Parasite were fixed with 3% formaldehyde, washed with FACS buffer (1X PBS with 1% FBS) before 4×10^5 fixed parasites were stained with the following primary antibodies (diluted in FACS buffer) on ice: α-TOXO terminal GalNAc T3 3F12 IgG3 (NR-50253, BEI) at 1:400; α-TOXO terminal glucose T5 4E10 IgM ascites (were generously gifted by Jean-François Dubremetz from the Université de Montpellier, France) at 1:100; α-P35 (SRS29C) T4 3F12 IgG2a (NR-50259, BEI) at 1:400. The parasites were washed with FACS buffer and then stained with the following detection antibodies at 1:100 in FACS buffer: α-IgM PECy7 RMM-1 (406514) [Biolegend], α-IgG3 BV421 R40-82 (565808) [B.D. Biosciences], α-IgG2a PerCPCy5.5 RMG2a-62 (407112) [Biolegend]. Parasite were washed and analyzed with a BD LSRII flow cytometer at the University of California, Merced Stem Cell Instrument Foundry. P35, a highly expressed surface SAG protein, expressing parasites (P35+>96%) were analyzed for T3 3F12 and T5 4E10 staining to infer specific isoforms of the *T. gondii* GPI side chain.

Table 1. Models and Cell Lines

Cell Lines and Parasites	Type	Strain Type	Species	Supplier
Human Foreskin Fibroblasts (HFF)	Host	N/A	*Homo sapien*	Jeroen Saeij, UC Davis
GT1	Parasite	I	*Toxoplasma gondii*	
RH*Δku80*	Parasite	I	*Toxoplasma gondii*	
CEP	Parasite	III	*Toxoplasma gondii*	
RH*Δku80ΔompdcΔup::HXGPRT*	Parasite	I	*Toxoplasma gondii*	N/A
RH1-1	Parasite	I	*Toxoplasma gondii*	
RH*Δku80Δ259530::HXGPRT*	Parasite	I	*Toxoplasma gondii*	N/A
A/J (000646)	Host	N/A	*Mus Musculus*	Jackson Laboratories
C57BL/6J (000664)	Host	N/A	*Mus Musculus*	Jackson Laboratories
Bumble (*Nfkbid* Null)	Host	N/A	*Mus Musculus*	Dr. Nicole Baumgarth; UC Davis

Table 2. Reagents

Reagent Name	Supplier	Catalogue Number
Pierce BCA Protein Assay Kit	ThermoFisher	PI23225
Pre-Cast SDS gradient gel (4-20%)	Biorad	4561096
PVDF Membrane Transfer Pack	Biorad	1704156
Precision Plus Dual Color Protein Standard	Biorad	161-0374
Goat α-mouse IgM- HRP	ThermoFisher	62-6820
Goat α-mouse Total IgG-HRP	Southern Biotech	1030-05
T5 4E10 α-Glucose Terminal IgM Ascite	Dubremetz	Gifted
T3 3F12 α-GalNAc Terminal IgG3 mAb	B.E.I.	NR-50253
T4 3F12 α-P35 IgG2a mAb	B.E.I.	NR-50259
α-IgM PECy7 (Clone: RMM-1)	Biolegend	406514
α-IgG3 BV421 (Clone: R40-82)	B.D. Biosciences	565808
α-IgG2a PerCPCy5.5 (Clone: RMG2a-62)	Biolegend	407112
Phosphatidylinositol-specific phospholipase C (PI-PLC) recombinant from *B. cereus*	ThermoFisher	P6466
β-N-Acetylhexosaminidase f	N.E.B.	P0721S
Jack-Bean α-Mannosidase isolated from *Canavalia ensiformis*	Sigma	9025-42-7
Illuminata Forte Western HRP Substrate	Millipore	WBLUF0500
One Shot TOP10 *E.coli*	Life Technologies	C4040-03
PSS013 Plasmid	Saeij Lab UC Davis	N/A
DNA Ladder 1Kb -Plus	ThermoFisher	10-787-018
TrizmaBase HCl	Sigma	T5941-500G
99% Glycerol	Alfa Aesar	AAAA16205-AP
Tween 20	Amresco	97062-332
Glycine HCl	Sigma	G2879-500G
Hydrochloric Acid	ACS	BDH3026-500MLP
Hydrofluoric Acid 48-51%	BDH	BDH3040-500MLP
DMEM+GlutaMAX Supplement	Gibco	10566024
FBS (Lot 463304)	Omega Scientific	FB-03
PBS (Sterile) pH 7.4	Gibco	10010049
Gentamycin	Millipore Sigma	G1397-100ML
Uracil	Sigma	U1128-100G

ATP	ThermoFisher	97061-226
L-Glutamine	Life Technologies	21051024
Ampicillin	ThermoFisher	BP176025
Penicillin/Strep Cocktail	ThermoFisher	15140122
TE Buffer	Invitrogen	12090-015
BME	Gibco	21985-023
Ethidium Bromide	Biorad	1610433
Mycophenolic Acid (MPA)	ThermoFisher	50-953-724
Xanthine	ThermoFisher	AAA11077-22
Plasmid Maxiprep Kit	Zymo Research	D4203
RNeasy Plus Mini Kit	QIAgen	74134
Mango Mix	Bioline	BIO-25034
Ethanol (100%, 70%)	Koptec	490000-610
DNAzol® Reagent	Invitrogen	10503-027
Bromophenol Blue	Amresco	97061-690
1X PBS (Sterile)	Gibco	10010049
Agarose	Biorad	1613102
Sodium Chloride	Amresco	0241-2.5KG
Trypan Blue 0.4%	Corning	45000-717
Methanol	BDH	BDH1135-4LP
Trypsin (2.5%)	LifeTechnologies	15090-046
Triton X100	Fisher	EM-TX1568-1
Formaldehyde 16%	Fisher	NC9864402
DMSO	BDH	BDH1115-1LP
EDTA	BDH	BDH9232-500G
Fortified Dry Milk	Raley’s	N/A
Bleach	NP&PC/ESSENDANT CO.	170094
pH Test Strips BDH 6-10	BDH	BDH83931.601
LB Agar	BD Difco	DF0445-17-4
LB Broth	BD Difco	DF0446-17-3
BsaI-HF	N.E.B.	R3535L
Quick Ligation Kit	N.E.B.	M2200L
BSA	N.E.B.	EM-2930
Calcium Chloride	Amresco	97062-590
Glutathion (GSH)	ThermoFisher	AAA18014-06
Sodium Hydroxide	BDH	BDH7247-1

Table 3. Equipment

Equipment Name	Supplier	Catalogue Number
Chemidoc Touch	Biorad	12003153
Transblot Turbo Transfer	Biorad	1704150
Thermocycler C1000	Biorad	1851148DEMO
Thermocycler T100	Biorad	1861096DEMO
Epoch Plate Reader	Biotek/Fisher	BTEPOCH
Electrophoresis Western Blot Cell	Biorad	1704402
Horizontal Electrophoresis System	Biorad	1704467
PowerPac Basic Power Supply	Biorad	1645050
Orbital Shaker	VWR	89032-088
Electroporator Gene Pulser Xcell CE	Biorad	1652667
Electroporator Cuvettes	Biorad	1652086
Chemidoc XRS+	Biorad	1708265
LSRII Flow Cytometer	BD	N/A
Hemacytometer	Fisher	02-671-55A
Heating Blocks	VWR	13259-286
Excella E24 Incubator Shaker	Eppendorf	R1352-0000
Isotemp Incubator	Fisher	1325525
Biosafety Cabinet	Fisher	302481100
Rocking Platform	VWR	40000-304
T25 Falcon Tissue Culture Treated Flasks	Fisher	10-126-9
T75 Falcon Tissue Culture Treated Flasks	Fisher	07-202-000
T175 Falcon Tissue Culture Treated Flasks	Fisher	10-126-13
Tissue Culture Plates 96 well	Fisher	087722C
Tissue Culture Plates 24 well	Fisher	087721
Petri Dishes	Fisher	08757100D
Disposable Syringes (5mL)	Fisher	1482945
Disposable Syringes (10mL)	BD Syringes	302995
Pipet Tips (all volumes)	USA Scientific	1121-3810, etc.
Serological Pipettes (all volumes)	VWR	490000-608, etc.
Needles (27G, 25G, 18G) BD Precision Glide	Fisher	1482648, etc.
Insulin Syringe U-100	Fisher	14-826-79
PCR Tubes (0.2mL)	USA Scientific	1402-4700
Conical Centrifuge Tubes 0.6mL	Fisher	14222143
Conical Centrifuge Tubes 1.5mL	Fisher	14222155
Conical Centrifuge Tubes 5mL	Fisher	14-568-100
Conical Centrifuge Tubes 15mL	Fisher	14-959-49B
Conical Centrifuge Tubes 50mL	Fisher	1495949A
Culture Tubes (14mL)	VWR	60818-725
Cryogenic Vials	Fisher	03-374-20
Glass Pasteur Pipets	Fisher	1367820D
Transfer Pipettes	Fisher	1371121
Rubber Policeman	Fisher	22261768

Table 4. Oligos for CRISPR and PCR Designs

Primers, Guides, Homology	Sequence (5'-3')	Supplier
C7b_259530_gRNA Fw	aagttGCTGAGTCCTAGTGCACg	IDT
C7b_259530_gRNA Rv	aaaacGTGCACTAGGACTCAGCa	IDT
C7b_259530_Fw Primer	TTTCTGCATTTCCCTGTCGCTACC	IDT
C7b_259530_Rv Primer	TTGACCCCCCTCGTATCCGAG	IDT
HPT_H-Arm259530_Fw	ATCGCGGAGACGCGTGTGGGcagcacgaaacc	IDT
HPT_H-Arm259530_Rv	GAGACAGGTCGTTAACAAAGgtgtcactgtagcctgccagaac	IDT
C1b_207750_gRNA_Fw	aagttGGAGGAGTCACATTCGGCGGg	IDT
C1b_207750_gRNA_Rv	aaaacCCGCCGAATGTGACTCCTCCa	IDT
C1B207750_Fw Primer	CGGTGACTGTCGTGAGAGCG	IDT
C1B207750_Rv Primer	AAAACGGCACAACACCTGCG	IDT
HPT_H-Arm207750_Fw	TGAGCACCTGGAAATGGTGGcagcacgaaacc	IDT
HPT_H-Arm207750_Rv	CGAACTCCCCTGCACATTCGgtgtcactgtagcctgccagaac	IDT
CIX_266320_gRNA_Fw	aagttCGCATGCTCAGGCTTGAGCGg	IDT
CIX_266320_gRNA_Rv	aaaacCGCTCAAGCCTGAGCATGCGa	IDT
CIX266320_Fw Primer	CTTCTTCGGTTGGCTCTCAGAATCG	IDT
CIX266320_Rv Primer	GTCTTCTTCCTCCTCTTCCTCACTG	IDT
HPT_H-Arm266320_Fw	GACGACGGAGAAGACGGAGCcagcacgaaacc	IDT
HPT_H-Arm266320_Rv	GACGAGGGAGAAGAAGGAAGgtgtcactgtagcctgccagaac	IDT
5370 HXGPRT Internal Primer	GCCGTAGTCTTCAATGGGTTTGG	IDT
5369(2018) HXGPRT Internal Primer	GTCTGGATCGTTGGTTGCTGC	IDT
PSS013 Primer Fw	5'- CAAATGGCGACCTGCAGAGG -3'	IDT

Table 5. Software and Algorithms

Software	Source	Identifier
FlowJo V10.1	FlowJo	N/A
Prism7	Graphpad	N/A
ImageLab	BioRad	N/A

Chapter 3

3. Results

3.1 Serum antibody reactivity to *T. gondii* lysate antigen is enhanced in resistant compared to susceptible mice

We first sought to determine whether genetically resistant A/J and susceptible B6 mice differ in their ability to produce parasite-specific antibodies to *T. gondii* lysate antigen, and whether such differences correlate with disease outcome (Figure 1). To do so, the model we use is to prime A/J and B6 mice with the Type III avirulent *T. gondii* strain CEP interperitoneally (IP) and allow them to progress to chronic infection. These mice were serotyped 30-35 days later for confirmation of seroconversion indicative of chronic infection (details in materials and methods; Figure 3 schematic). From here, half of the cohort (n=6-10 for each mouse strain) was challenged (n=3-5) with the virulent Type I GT1 strain, which generates a lethal infection in B6 but is controlled in A/J mice (Figure 1A and B), and the other half was not challenged. Serum harvested from chronically infected mice or mice on day 5 of challenge (Figure 3 schematic) and used to probe antibody reactivity to Type I GT1 *T. gondii* lysate antigen separated on SDS-page and analyzed by western blot. We found A/J and B6 serum antibody had similar antigen reactivities with heavy preference for antigens less than 50kDa in both chronic and day 5 challenge conditions (Figure 4A and D). From visual assessment of the banding patterns between mouse strains, it appeared that A/J produced more specific serum IgM and total IgG antibody against *T. gondii* proteins. To quantify this observation, the total signal intensity generated in a single

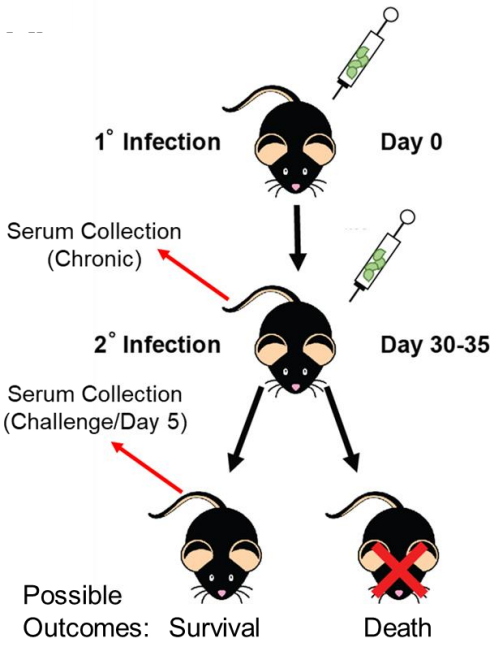

Figure 3. Infection model. *Primary infection with Type III CEP was administered IP and allowed to progress to chronic infection condition (30 days). A secondary challenge with virulent Type I GT1 was administered IP and allowed to progress for five days before mice were euthanized. Serum collections performed as either tail bleed or terminal collection (see materials and methods).*

lane was measured across all blots and experiments (as described in materials and methods). While there was not a significant difference between mouse strains (unpaired student's t-test $P>0.05$), on average, serum-derived antibodies from A/J generated greater total lane signal compared to B6 (Figure 4B and E). Since A/J and B6 serums are developed simultaneously within respective detection antibody classes we normalized the total lane signal of B6 to that of A/J (A/J = 1) (see material and methods), to allow comparison across multiple experiments and to minimize variance introduced by imaging at different timepoints, . Using normalized values, the total lane signal was significantly less for B6 compared A/J serum from day 5 challenged mice for both IgM (Figure 4G) and total IgG reactivity (Figure 4H) (paired student's t-test IgM $P=0.03$, IgG $P=0.002$). Serum from chronically infected mice generated non-significant differences (Figure 4G, 4H). These results suggest host resistance correlates with enhanced production of parasite-specific antibodies during a secondary infection.

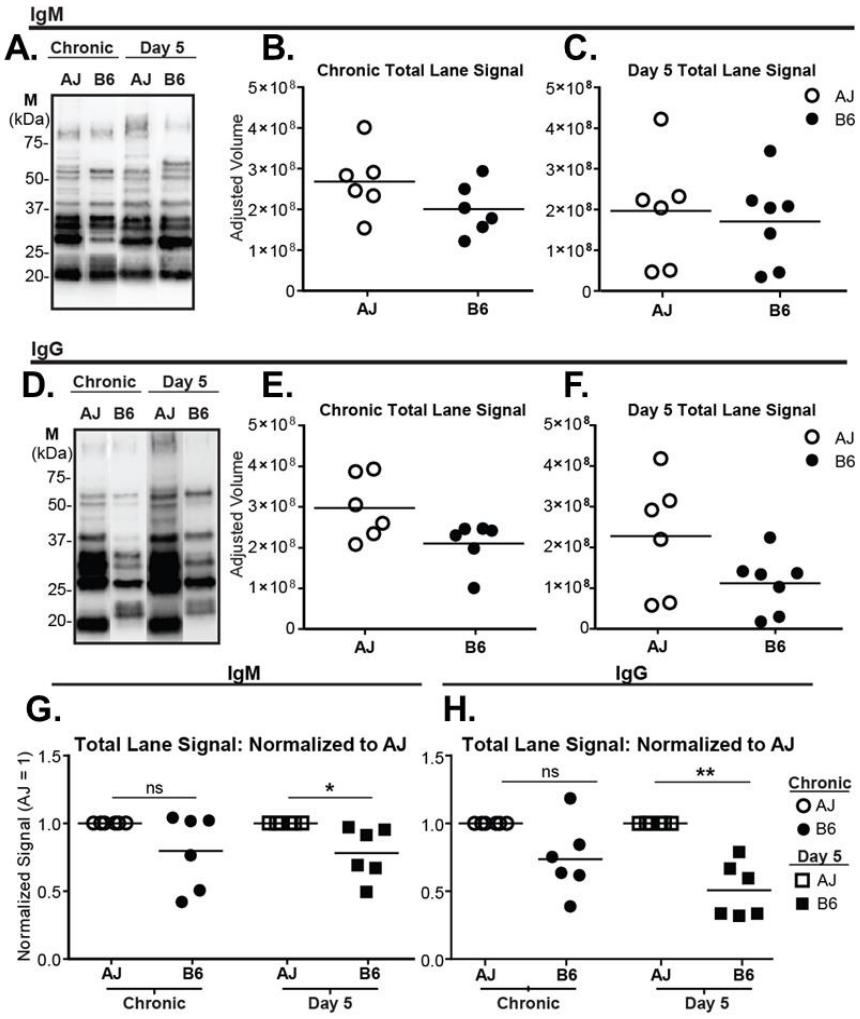

Figure 4. Serum antibody reactivity to T. gondii lysate antigen is enhanced in A/J compared to C57BL/6J mice. A. *Western blot: serum harvested from chronically infected or from day 5 Type 1 GT1 challenged A/J and B6 mice was used as a primary detection probe of reduced GT1 lysate separated by 4-20% gradient SDS-PAGE. Goat α-mouse IgM horseradish peroxidase (HRP)-conjugated secondary antibody probed for serum IgM. Blots using A/J and B6 serums, were treated, developed and imaged simultaneously to reduce exposure variability; a representative image is shown.* ***B.*** *Total lane signal ('adjusted volume') probed with serum from chronically infected mice.* ***C.*** *Total lane signal probed with serum from mice on day 5 of challenge.* ***D.*** *Western blot as described in A, but goat α-mouse total IgG HRP-conjugated secondary antibody probed for total serum IgG.* ***E-F.*** *As stated in B-C.* ***G-H.*** *Total lane signal of B6 normalized to A/J (A/J = 1) within serum conditions is plotted. For all graphs, each dot represents the results obtained from one mouse (n=6-7) taken from three individual experiments. Unpaired student's t-test between non-normalized A/J and B6 within serum conditions and between chronic and day 5 serum within mouse strains were non-significant P>0.05. Paired student's t-test between normalized A/J and B6 Day 5 and chronic serums produced significant values, P<0.05.*

3.2 B-1 cells may be responsible for a large portion of *T. gondii*-specific antibody: Bumble (*Nfkbid* null) mice generate significantly less antibody to *T. gondii lysate antigen*.

Previous work done by our lab suggests that *Nfkbid* plays an important role in survival of secondary infection with *T. gondii* (Souza, S., unpublished; Figure 1A) and is required for the generation of the majority of IgM and IgG parasite-specific antibodies (Souza, S unpublished, not shown). To extend these findings to *T. gondii* lysate antigen, we utilized serum from chronically infected *Nfkbid* null bumble mice (C576BL/6 background), which are deficient in B-1 cells but not B-2 cells (Arnold et al., 2012; Pedersen et al., 2016; Touma et al., 2011). In keeping with our infection model, bumble and control C57BL/6 mice were primed IP with a Type III avirulent *T. gondii* strain CEP and serum from chronically infected mice serum was used to probe *T. gondii* lysate antigens via western blot (Figure 5 A and D). In this configuration, lysates were generated from the three different strains of *T. gondii* used in our system, (left to right) GT1, RH *Δhxgprtku80* and CEP, and loaded at the same protein concentrations (measured as mentioned in material and methods) to minimize variability between lysates. In all, bumble mice were highly defective in generating antibodies to parasite lysate antigen and, compared to wild type B6 serum (*$P<0.05$), produced an average of 91% for IgG and 87% for IgM less reactivity to lysate antigen (Figure 5 C and E). One-way ANOVA comparing antibody reactivity to the different parasite strains was not significant ($P>0.05$) indicating antibody recognition of the strain types is generally conserved. In summary, these results are consistent with our previous unpublished observations that bumble (*Nfkbid* null) susceptibility to secondary infection correlates with a general defect in generating parasite-specific antibodies (Figure 1).

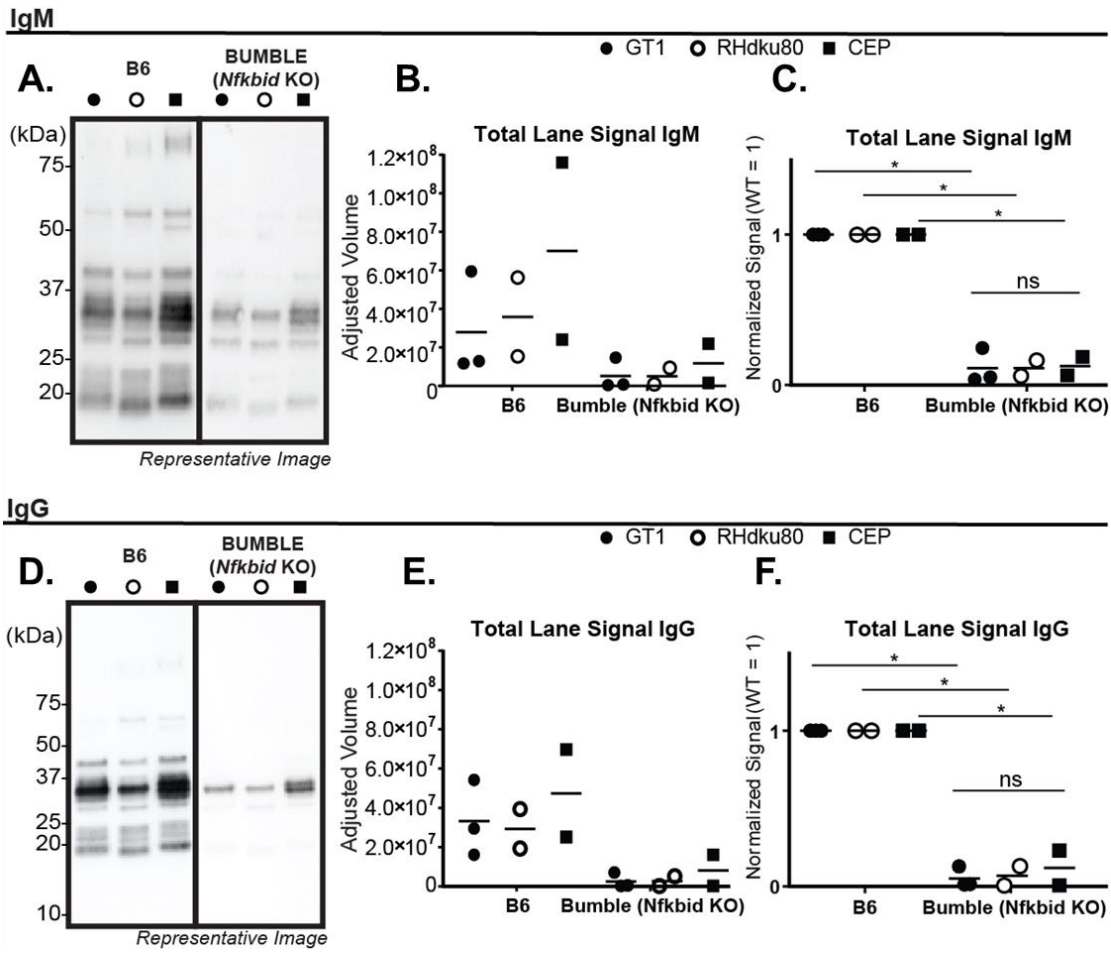

Figure 5. Nfkbid is required for generating T. gondii-specific antibody to lysate antigen. A. *Western blot: serum harvested from chronically infected B6 and Bumble (Nfkbid null) mice was used as a primary detection probe of reduced GT1, RHΔku8 and CEP lysate separated by 4-20% gradient SDS-PAGE. Goat α-mouse IgM HRP-conjugated secondary antibody probed for serum IgM; a representative image is shown.* ***B.*** *Total signal intensity ('adjusted volume') for each condition is plotted.* ***C.*** *Total lane signal of Bumble was normalized to that of B6 (B6 = 1) and plotted.* ***D.*** *Western blot as described in A but using goat α-mouse total IgG HRP-conjugated secondary antibody.* ***E-F.*** *As described in B-C. Each dot represents the result from an individual mouse from 2 to 3 separate experiments. Unpaired student's t-tests were non-significant for non-normalized values (B and E). Paired student's t-test comparing bumble normalized to B6 was significant for each parasite lysate P<0.05 (C and F). One-way ANOVA comparing signal intensity differences generated against the different parasite strains was non-significant (B,C,E,F).*

3.3 Hypothesis: A/J and B6 serum antibodies heavily target the GPI anchor of surface antigens.

Assessment of the heavy targeting by both A/J and B6 serum antibodies indicated antigens below 50kDa were of importance (Figure 3 A and D). Additionally, bumble mice are largely incapable of detecting these same antigens (Figure 4). The B-1 cell population absent in Bumble mice produce antibody against ubiquitous pathogen- and self-antigens (Baumgarth, 2011) which suggest the moiety responsible for antibody recognition may be conserved and non-protein in nature. Based on the molecular weight of the targeted bands in Figure 4, we suspected the identity of many of these antigens to be GPI anchored surface proteins (Table 6) (Manger et al., 1998; Tomavo et al., 1989). Due to the sugar composition and kingdom-conserved core structure of the GPI anchor (Figure 2)(Ferguson, M. A., Low, M. G., and Cross, 1985; Ferguson, 1999; Homans et al., 1988; Low, M., Hoessli, D. C., and Ilangumaran, S., 1999; Nosjean, O., Briolay, A., and Roux, 1997), we hypothesize the GPI anchor is a likely candidate for B-1 cell antibody targeting.

Protein Label	Alternative Identifiers	Gene I.D. (ToxoDB.org)	Molecular Weight	Known Functions	Reference
P46	SRS29A	TGGT1_233450	46kDa	Polymorphic between RH and GT1$^{\Delta}$	Yang et al. 2013
P43	SAG3, SRS57	TGGT1_308020	43kDa	Host cell adhesion; virulence$^{\beta}$	Cesbron-Delauw et al 1994
P35	SRS3, SRS29C	TGGT1_233480	35kDa	Attenuates virulence†, Polymorphic between RH and GT1$^{\Delta}$	Manger et al 1998; Wasmuth, et al. 2012; Yang et al. 2013
P30	SAG1, SRS29B	TGGT1_233460	30kDa	Host cell invasion; IFNγ modulator$^{\kappa}$	Burg et al. 1988; Cong, et al. 2005
P22	SAG2A, SRS34A	TGGT1_271050	22kDa	Modulates IL-1β in macrophage$^{\alpha}$	Prince et al 1990

Table 6. Several immunogenic T. gondii proteins below 50kDa are known to be GPI anchored to the outermost parasite membrane*. This table was adapted from Lekutis, Ferguson, Grigg, Camp and Boothroyd (2001) and shows a truncated list of SAGS or SAG1-Related Sequence (SRS) proteins of interest (Ref. α Leal-Sena, et al. 2018; β Dzierszinski, et al. 2003; κ Lekutis, et al. 2001; Δ Yang, et al. 2013; † Wasmuth, et al. 2012). Gene I.D.'s listed are for GT1 strain and are current as of March 2019.*

3.4 Both A/J and B6 serum antibodies require the lipid portion of the GPI anchor for maximal reactivity to *T. gondii* lysate antigen

To determine whether serum antibodies predominantly target the GPI anchor, we first began by dismantling a piece of the GPI anchor: the lipid alkyl-glycerol tail (Figure 8A). Phosphatidylinositol specific phospholipase C (PI-PLC) is known to cleave the phosphate bond linking the inositol group to the alkyl-glycerol group imbedded in the membrane. Original work done by others with the parasite *Trypanosoma* s.p.p., revealed these components of the GPI anchor via the exposure of a common reactive determinant (CRD) region which exposes the inositol group of the GPI anchor (Ferguson et al., 1988). This method had been replicated by several groups in the confirmation of protein linkage to the surface of *T. gondii* (Manger et al., 1998; Nagel and Boothroyd, 1989) but use of PI-PLC has not been attempted to asses serum antibody recognition of parasite lysate antigen. Importantly, when we treated parasite lysate with PI-PLC and probed with serum (as previously described) approximately 70% of the total lane signal previously seen in Figure 4 was lost for both IgM (Figure 6) and IgG (Figure 7). This was true for serum derived antibodies from chronically infected and day 5 challenged mice. Therefore, antibody recognition of *T. gondii* lysate antigen is highly dependent on an intact GPI anchor.

3.4.1 IgM serum antibody reactivity to antigens below 50kDa requires the GPI lipid moiety

We further evaluated the dependence of serum IgM antibody on the lipid moiety of the GPI anchor in greater detail (Figure 6). In the chronic condition as mentioned above, the total lane signal was significantly reduced for both A/J and B6 in response to PI-PLC treatment of lysate (paired student's t-test $P<0.05$) indicative of high dependence on the lipid moiety for serum IgM reactivity to lysate antigen (Figure 6E). However, a comparison between A/J versus B6 antibody-probed treated lysate demonstrated no significant difference in the abrogation of the total western blot signal between the two mouse strains (unpaired student's t-test $P<0.05$) (Figure 6E). Narrowing our focus to individual antigens marked by arrows (Figure 6A), we found the majority of signal below 50kDa to be significantly sensitive to PI-PLC treatment for both mouse strains, particularly P43, P34, P33-32, P30 and P22 (paired student's t-test of normalized treated v. untreated; $P<<0.0001$) with less of an effect for P46 and P35 molecular weight antigens (paired student's t-test: A/J $P<0.05$, B6 non-significant) (Figure 6B). It's important to note bands 50kDa and higher are not impacted by PI-PLC treatment in the same way, which suggests these antigens are either not GPI-anchored proteins or lipid removal does not impact antibody recognition. For

chronically infected A/J and B6 mice, serum IgM does not differentially target the GPI anchor of any single antigen between mouse strains (unpaired student's t-test $P>0.05$).

Similar results were obtained with serum from day 5 challenged mice with a few subtle differences (Figure 6C). Total lane signal assessment of each mouse strain revealed a significant quantitative difference in treated versus untreated probed lysate (paired student's t-test $P<<0.0001$) (Figure 6F). In contrast to analysis of chronic serum, A/J produces slightly more serum IgM on day 5 of challenge that is refractory to PI-PLC treatment compared to B6 (unpaired student's t-test $P=0.002$). Moreover, analysis of individual antigens reveals day 5 serum IgM from A/J is slightly less dependent on the lipid moiety for the P34 and P30 antigens than B6 (unpaired student's t-test $P=0.003$ and $P=0.00004$, respectively). Whether reduced targeting of the GPI anchor of P30 (likely SAG1, Table 6 above) underscores A/J immunity to *T. gondii* is unknown but may imply a balanced repertoire of antibodies that recognize both protein and GPI epitopes of *T. gondii* SAGs is necessary to survive virulent challenge.

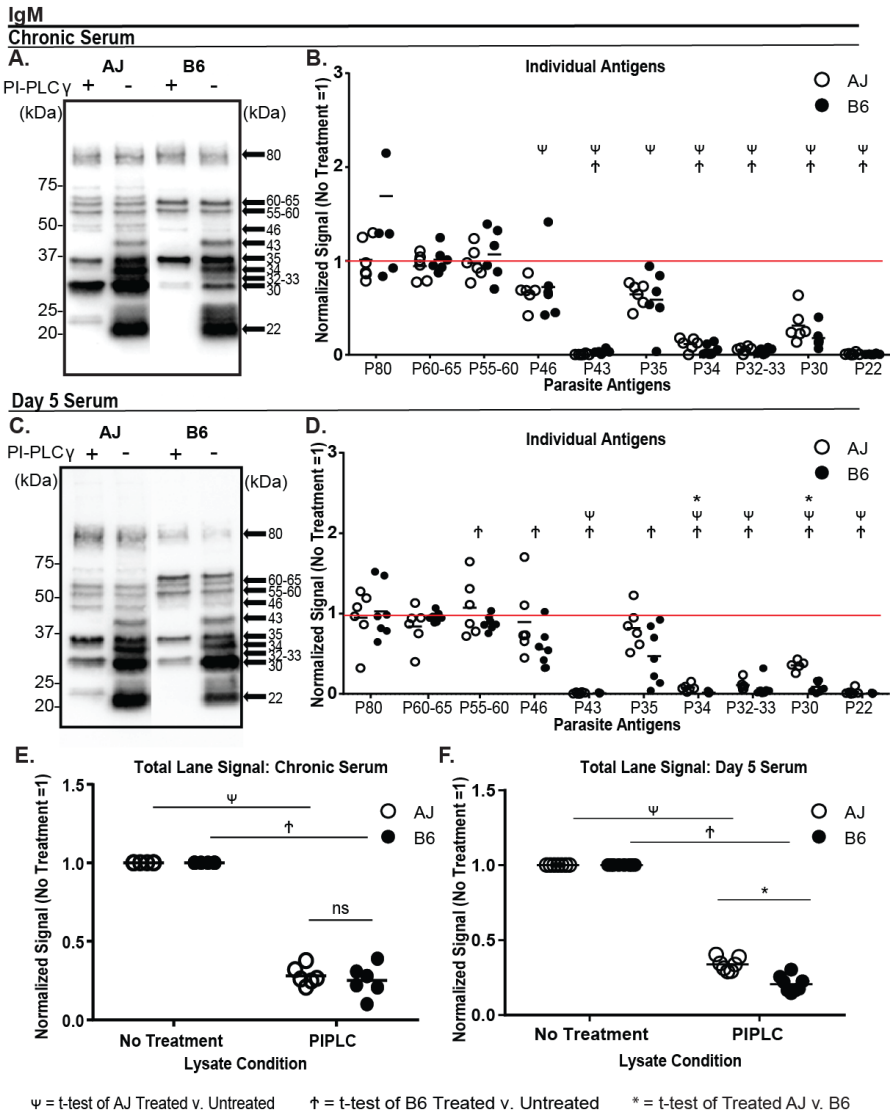

Figure 6. A/J and B6 serum IgM relies heavily on the lipid tail of the GPI anchor for detection of T. gondii lysate antigen. A. *Representative western blot of T. gondii lysate antigen probed with serum from chronically infected A/J and B6 mice and detected with anti-IgM; (as previously described); detection of PI-PLC- treated and mock-treated GT1 lysate is analyzed. Arrows indicate prominent individual bands of interest with corresponding molecular weights.* ***B.*** *Quantification of individual bands of interest (A) following PI-PLC treatment and normalized to mock treated band intensities (mock=1).* ***C.*** *As in A, but serum from challenged (Day 5) A/J and B6 mice was used.* ***D.*** *Quantification of bands (C) as previously described.* ***E.*** *Total lane signal of chronic serum-probed PI-PLC normalized to mock treated T. gondii lysate (mock = 1).* ***F.*** *Total lane signal of challenge (Day 5) serum-probed PI-PLC normalized to mock treated parasite lysate (as described in E). For all graphs, each dot represents the results from one mouse (n=6-7) obtained from three separate experiments (n=3). Ψ paired student's t-test normalized A/J treated v. non-treated (most P<0.0001). † paired student's t-test B6 normalized treated v. non-treated (most P<0.0001). * unpaired student's t-test normalized PIPLC treated A/J v. treated B6 (P<0.05). Detailed statistical significance can be found in Table 7.*

3.4.2 Total IgG serum antibody reactivity to antigens below 50kDa requires the GPI lipid moiety

We further analyzed total IgG reactivity to lysate antigen (as previously stated) and found a near identical trend to that of IgM (Figure 7A, B, E). Serum IgG antibody reactivity to lysate antigen from chronically infected A/J and B6 mice was significantly reduced for both A/J and B6 in response to PI-PLC treatment of lysate (paired student's t-test $P<0.05$) (Figure 7E). A/J versus B6 antibody-probed treated lysate total lane signal demonstrated no significant difference in the abrogation of total lane signal between the two mouse strains (unpaired student's t-test $P<0.05$) (Figure 7E). Individual antigens, marked by arrows (Figure 7A), when quantified and normalized demonstrated the majority of signal below 50kDa to be significantly lost following PI-PLC for both mouse strains. Again, antibody reactivity to P43, P34, P33-32, P30 and P22 were particularly sensitive to PI-PLC treatment (paired student's t-test $P<<0.0001$) (Figure 7B). One subtle difference noted between isotype classes is that PI-PLC impacts IgG antibody detection of the P46 and P35 antigens more consistently than for IgM. As with IgM, bands 50kDa and higher detected by IgG are not impacted by PI-PLC treatment in the same way as bands below. For chronically infected AJ and B6 mice, serum IgG differentially targets only one antigen between mouse strains: P30 (putatively SAG1) (unaired student's t-test $P<0.05$).

Following challenge (Day 5), total IgG produced similar results to that of IgM (Figure 7C, D, F). PI-PLC treatment abrogates the majority of IgG antibody detection of lysate antigen for both B6 and A/J (paired student's t-test $P<0.0001$), with A/J being less sensitive to treatment compared to B6 (unpaired student's t-test $P=0.002$) (Figure 7F). Loss of the lipid moiety epitope significantly impacts recognition of all antigens of interest below 50kDa in both mouse strains in the chronic as well as the challenge condition. Just as analysis of IgM following challenge revealed only two antigens which are differentially targeted between A/J and B6, analysis of total IgG in the challenge condition found the same two antigens, (i.e. P34 and P30) to elicit statistically different antibody reactivity following PI-PLC treatment (unpaired student's t-test $P<0.05$) (Figure 7D). Thus, as with IgM, IgG produced against *T. gondii* heavily relies on the lipid moiety for recognition. In summary, we hypothesize that A/J produces more parasite-specific IgM and IgG antibody compared to B6, as implicated in section 3.1, but these antibodies display broader coverage against epitopes found within the *T. gondii's* SAGs, thus affording more protective antibody response upon re-exposure.

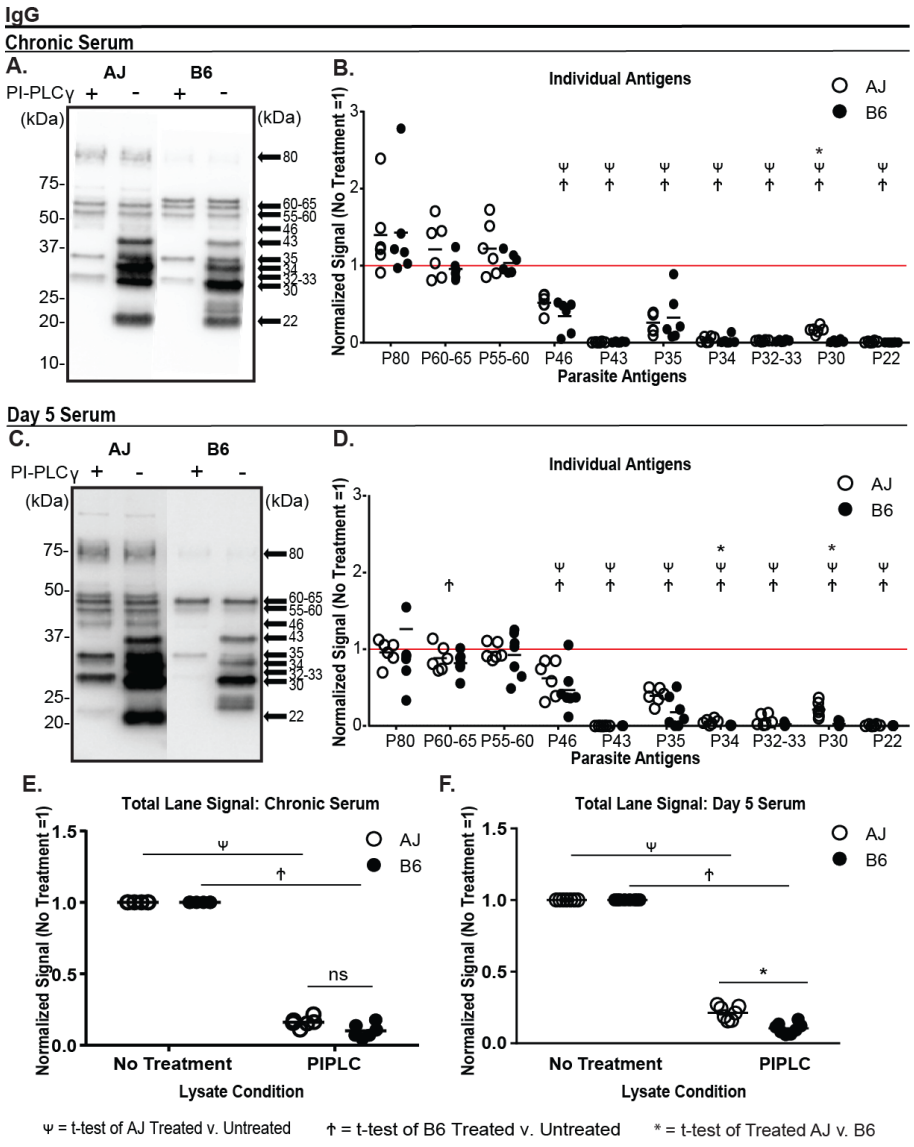

Figure 7. A/J and B6 serum IgG relies heavily on the lipid tail of the GPI anchor for detection of T. gondii lysate antigen. A. *Western blot of chronic serum IgG from A/J and B6 mice (as previously described); detection of PI-PLC treated GT1 lysate. Arrows indicate prominent individual bands of interest with corresponding molecular weights.* ***B.*** *Quantification (as previously described) of individual bands of interest (A) normalized to mock treated bands.* ***C.*** *Western blot using serum from challenged (Day 5) A/J and B6 mice; developed as previously stated in A.* ***D.*** *Quantification of bands (C) as previously described in B.* ***E.*** *Total lane signal of chronic serum-probed PI-PLC normalized to mock treated T. gondii lysate (mock = 1).* ***F.*** *As in E, but challenge (Day 5) serum is used. For all graphs, each dot represents one mouse from three individual experiments (n=3). Ψ paired student's t-test normalized A/J treated v. non-treated (most P<0.0001). † paired student's t-test B6 normalized treated v. non-treated (most P<0.0001). * unpaired student's t-test normalized PI-PLC treated A/J v. B6 (P<0.05). Detailed statistical significance can be found in Table 7.*

A

	Chronic Serum IgM						Day 5 Serum IgM					
	AJ (Treated v. Non-Treated)		B6 (Treated v. Non-Treated)		AJ v. B6 (Treated v. Treated)		AJ (Treated v. Non-Treated)		B6 (Treated v. Non-Treated)		AJ v. B6 (Treated v. Treated)	
Individual Band	Significant?	P value	Significant?	P value	Significant?	P value	Significant?	P value	Significant?	P value	Significant?	P value
P80		0.913694		0.144278		0.156874		0.730082		0.836182		0.693731
P60-65		0.346222		0.839876		0.412159		0.146446		0.0901418		0.252809
P55-60		0.752042		0.543794		0.496712		0.625529	**	0.005423		0.201585
P46	***	0.000219		0.0882447		0.727135		0.578831	***	0.0005239		0.11812
P43	****	7.04E-22	****	1.000E-16		0.0157411	****	5.005E-20	****	3.026E-25		0.643736
P35	****	3.777E-05		0.0104485		0.708233		0.109304	****	0.0019756		0.0717409
P34	****	1.281E-11	****	3.357E-12		0.134542	****	1.314E-13	****	2.070E-22	**	0.003456
P33-32	****	4.595E-15	****	3.778E-15		0.343425	****	1.549E-11	****	4.421E-11		0.443115
P30	****	2.389E-06	****	8.928E-09		0.159697	****	1.196E-09	****	2.277E-13	****	4.843E-05
P22	****	2.845E-19	****	1.147E-22		0.372319	****	2.472E-14	****	3.337E-26		0.234263

B

	Chronic Serum IgG						Day 5 Serum IgG					
	AJ (Treated v. Non-Treated)		B6 (Treated v. Non-Treated)		AJ v. B6 (Treated v. Treated)		AJ (Treated v. Non-Treated)		B6 (Treated v. Non-Treated)		AJ v. B6 (Treated v. Treated)	
Individual Band	Significant?	P value	Significant?	P value	Significant?	P value	Significant?	P value	Significant?	P value	Significant?	P value
P80		0.091011		0.153145		0.929174		0.564601		0.52399		0.666307
P60-65		0.190396		0.499624		0.14836		0.10961	**	0.005915		0.464538
P55-60		0.15325		0.523829		0.25182		0.443362		0.515916		0.762462
P46	****	1.001E-06	****	1.513E-05		0.102924	**	0.002521	***	0.000420		0.324622
P43	****	1.589E-22	****	5.92E-22		0.432294	****	2.237E-31	****	2.182E-34		0.240571
P35	****	8.79E-08	***	0.0004		0.649255	****	4.891E-08	****	1.384E-07		0.0364124
P34	****	2.165E-14	****	7.986E-13		0.639446	****	1.498E-14	****	8.807E-28	**	0.003836
P33-32	****	8.669E-22	****	8.846E-19		0.586475	****	2.079E-11	****	3.999E-21		0.0874861
P30	****	8.694E-13	****	6.029E-18	****	2.419E-05	****	3.360E-09	****	6.805E-18	**	0.0005867
P22	****	3.008E-20	****	2.097E-29		0.0975205	****	5.085E-20	****	1.221E-33		0.131688

Table 7. Student's t-tests of individual western blot bands. A. *Individual bands detected by chronic or challenge serum IgM from A/J and B6 mice displayed in Figure 5B and D.* ***B.*** *Individual bands detected by chronic or challenge serum total IgG from A/J and B6 mice displayed in Figure 6B and D. For all serum antibody class conditions, A/J and B6 columns represent P values calculated in Prism using paired student's t-test as previously described. Similarly, A/J v. B6 columns represent P values calculated by unpaired student's t-test in Prism. Significant = P<0.05.*

3.5 Alternative attempts at GPI anchor disruption provide inconclusive results.

In an effort to dismantle the GPI anchor in different ways, we attempted three additional enzymatic or chemical methods to do so—each disruption aimed at a different portion of the anchor. In Figure 8, we illustrate for each strategy which chemical bond is supposed to

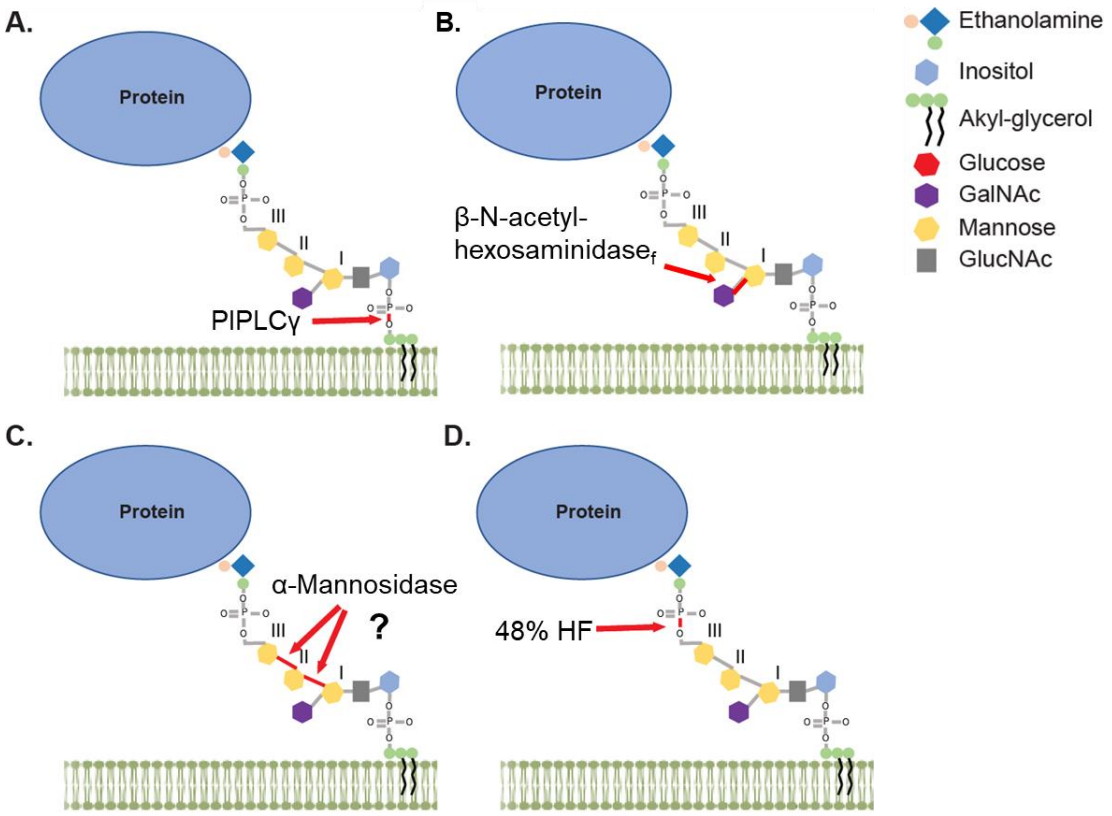

Figure 8. GPI disruption strategy to assess differential binding targets of antibodies from resistant and susceptible mice. A. *Phosphatidylinositol-specific phospholipase C cleaves at inositol-bound phosphate from lipid anchor.* ***B.*** *β-N-acetylhexosaminidase cleaves a terminal GalNAc when β1-6 or β1-4 linked to another sugar group.* ***C.*** *Jack Bean α-Mannosidase cleaves terminal mannose groups.* ***D.*** *48% Hydrofluoric Acid breaks ethanolamine-bound phosphate from the mannose backbone. For all illustrations, a red bar indicates the targeted single covalent bond.*

break. However, the results of the following GPI disruption strategies were largely found to be inconclusive due to technical limitations.

As previously mentioned, GPI anchored proteins of *T. gondii* have two GPI glycoforms which differ by the presence or absence of a single glucose addition to the β-GalNAc side chain off the first mannose of the carbohydrate backbone. In isolated deproteinated GPI's, the isoform with a terminal glucose has been shown to be more immunogenic than a terminal β-GalNAc (Gçtze et al., 2014; Striepen et al., 1997). In an effort to ascertain the dependence of serum antibody in our model on this side chain, we used β-N-acetylhexosaminidase to cleave terminal β-GalNAc from the GPI anchor (Striepen et al., 1992). Because we used GT1 lysate, derived from parasites grown in HFFs which generates a higher proportion parasite protein bearing the terminal β-GalNAc side chain GPI glycoforms (Azzouz et al., 2006), we anticipated a loss of serum recognition of lysate antigen following β-N-acetylhexosaminidase treatment if the antibody repertoire focused on this side-chain modification. However, use of this enzyme in our hands showed no measurable loss of signal was observed (data not shown). These results may support our model displays a lack of recognition of the terminal β-GalNAc glycoform. Alternatively, the β-N-acetylhexosaminidase has not been shown to cleave a proteinated GPI anchor which may ultimately inhibit enzymatic digestion. In these conditions, we would need further biochemical analysis to confirm enzymatic digestion of the side chain in the presence of an attached protein. Whether the side chain is preferentially targeted remains to be conclusively determined.

Another technique we utilized to disrupt the GPI moiety was treatment of our separated and PDVF transferred lysate with 48% hydrofluoric acid (HF). In other labs, 48-51% HF has been used to deproteinate purified GPI anchors by severing the ethanolamine-bound phosphate from the mannose backbone (Menon et al., 1990). Though others have reported HF treatment fails to hydrolyze peptide bonds, adjust molecular weight and/or alter immunochemical properties (Greenberg et al., 1992), we were still concerned this treatment would still destroy lysate antigens, change migration patterns in the SDS gel and/or at the very least, dilute lysate diminishing signal. Thus, after protein transfer, the PDVF membrane was bathed in HF for various periods of time to hydrolyze the ethanolamine bond prior to probing with immune serum and detection antibodies. With this method, we expected HF to separate the mannose backbone and to be subsequently washed away with the remainder of the GPI structure while the proteins would stay attached to the PVDF. Membranes bathed in PBS served as a control. Given our previous results that an intact GPI anchor was required for antibody recognition of the majority antigens below 50kDa (Figure 6-7), we anticipated a similar result following HF treatment. However, our results were uninterpretable, as the signal of the dual-purpose molecular weight marker standard (M) decayed in response to the HF treatment (Figure 9B). Quantification of two of the visible marker proteins (at 50kDa and 37kDa) demonstrated a decreasing signal (with respect to PBS treatment) with the increase of time spent in the HF bath. Because of this, we determined that this

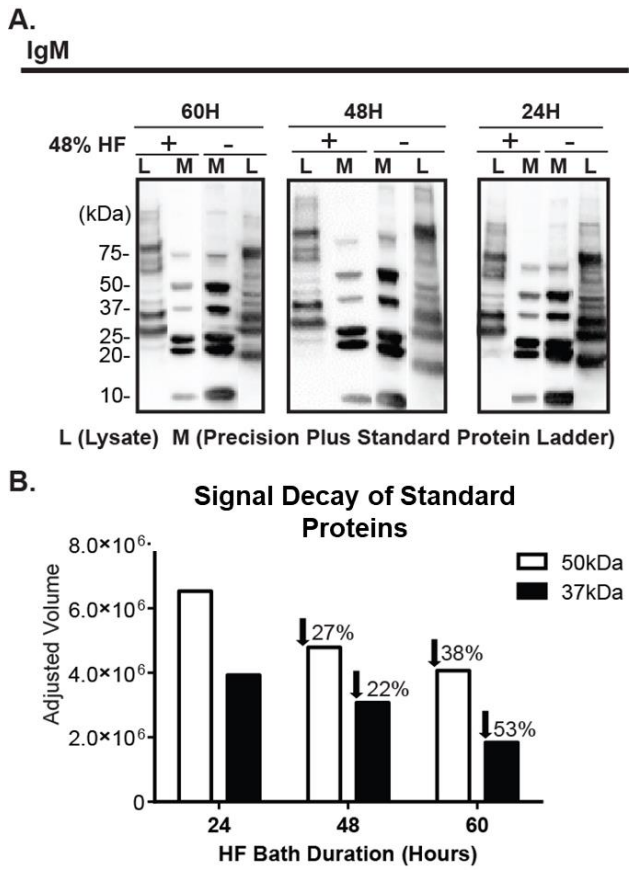

Figure 9. Hydrofluoric acid treatment of lysate on PVDF proves inconclusive due to compromise of internal standard. A. *Representative western blot of T. gondii lysate probed with immune serum and detected with anti-mouse IgM. Before serum probe, each blot was bathed in 48% HF for 24, 48 or 60 hours and neutralized in diH_2O and then PBS.* ***B.*** *Quantification of adjusted volume signal of 50kDa and 37kDa standard protein bands at 24, 48 and 60 hours. n=1.*

approach does not have the control needed to appropriately analyze these data. For that reason, we chose not to move forward with this approach.

We also attempted to disrupt the integral mannose backbone via Jack Bean α-mannosidase which was used in early works to extrapolate the structure of the GPI anchor in trypanosomes (Ferguson et al., 1988; Homans et al., 1988; Mayor et al., 1990b, 1990b, 1990a; Menon et al., 1990) and has been used exhaustively in previous study of *T. gondii* GPI glycoforms (Striepen et al., 1992; Tomavo et al., 1992c, 1992b, 1992a, 1992d). Jack

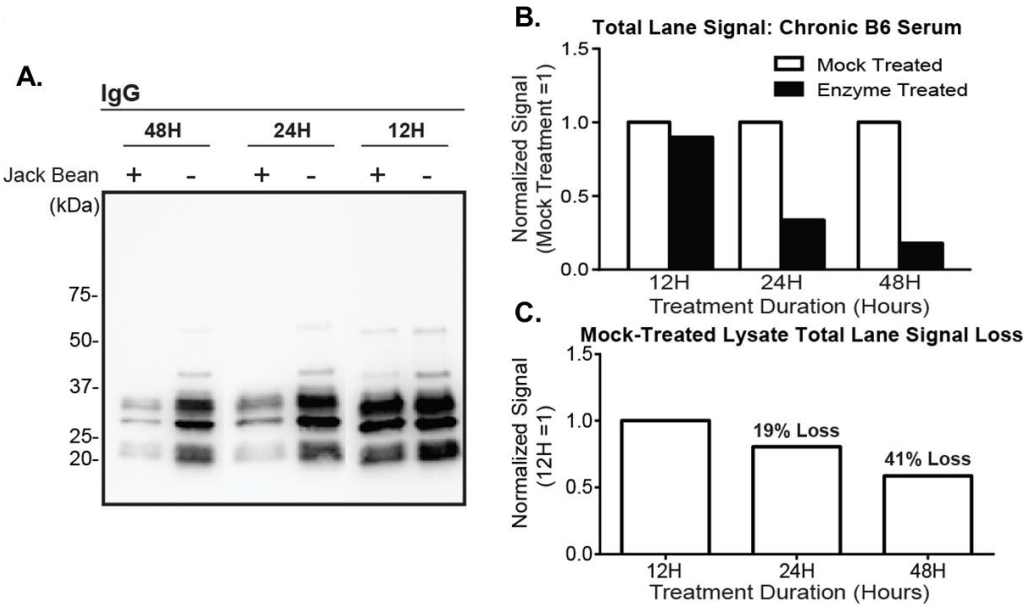

Figure 10. Jack Bean α-Mannosidase treatment of lysate was inconclusive due to overall degradation of sample. A. *Western blot of T. gondii lysate antigen probed with immune serum and detected with anti-mouse IgG. Lysate was treated with jack bean α-mannosidase: comparison at 12, 24 and 48 hours.* ***B.*** *For each time point, total lane signal of lysate treated with α-mannosidase was normalized to mock treated total lane signal.* ***C.*** *Mock treated total lane signal normalized to 12-hour mock treated total lane signal. n=1.*

Bean α-mannosidase cleaves terminal mannose so, our expectations were not high for this treatment simply because the various molecular weight antigens less then 50kDa were likely SAG antigens attached with the GPI anchor, thus leaving no terminal mannose sugars for enzymatic digestion. However, we found a decrease in signal from treated lysate at all time points chosen (Figure 10A and B). That said, the α-mannosidase treatment appeared to decrease the signal of the entire lane rather than individual bands as was observed with PI-PLC treatment. We noted the total lane signal of the mock treated lysate decayed nearly proportionate to the duration of time spent in buffer under mock conditions (Figure 10C). The result of this single experiment suggests our condition renders α-

mannosidase an inappropriate treatment for the analysis of antibody epitope in our mode—though future troubleshooting may resolve these concerns.

3.6 Deleting putative genes encoding the enzyme responsible for generating the side chain of both *T. gondii* glycoforms.

In an effort to remove the side chain of the *T. gondii* GPI isoforms, we began the search for the parasite enzyme responsible for adding the side chain. Although previous works by others suggested the existence of such an enzyme (Ferguson, 1999), the identity of this gene has yet to be made. Recently in humans, such an enzyme has been identified as PGAP4 which adds a β-GalNac to the first mannose of the carbohydrate backbone, however no clear homolog exists in the *T. gondii* genome (Hirata et al., 2018). Regardless, characteristics of PGAP4 provided clues to inform a search for an equivalent enzyme in *T. gondii* (described in materials and methods). Briefly, we looked for glycosyl transferases with a transmembrane that had a DXD or EDD motif, and ranked them based on their gene expression, presence of the EDD motif (part of the catalytic triad of PGAP4), and whether they were not associated with other irrelevant biological functions (i.e. tRNA synthetase); GPI synthetic pathway of the conserved core received a low rank. Gene text searches were performed on the ME49 strain background because it is the most fully annotated *T. gondii* genome. The results of this search can be seen in Table 8. Our initial attempts at gene selection were less refined than the approach previously mentioned which is why in the subsequent section, gene candidate TgME49_259530 ranked tenth in the table, was chosen for CRISPR editing. CRISPR editing of TGME49_266320, the number one rank, is currently underway.

Gene ID	Product Description	NonSyn/Syn SNP Ratio	No. TM Domains	Expressed?	EDD	Signal Peptide	∓ Mean Phenotype	Biologically Correct?	SUM
TGME49_266320	Domain with glycosyltransferase sugar-binding region containing DxD motif, has EDD motif	2.58	2	1	1	1	-0.99	1	4
TGME49_207070	Glycosyl transferase, putative ALG14 domian with UDP-N-acetylglucosamine transferase capacity for N-linked glycolsylation	1.77	2	1	0	1	-2.63	1	3
TGME49_246982	ALG11 mannosyltransferase N-terminus, involved in N-linked oligosaccharide synthesis and branching mannose side chains	1.22	1	1	0	1	-2.7	1	3
TGME49_203970	Dolichyl-diphosphooligosaccharide protein glycosyltransferase, putative N-linked glycolsylation in the ER	1.5	1	1	0	0	-4.25	1	2
TGME49_216540	Dolichyl-phosphate beta-glucosyltransferase, using UDP-glucose to make dolichyl beta-D-glucosyl phosphate	2.48	2	1	0	0	-3.36	1	2
TGME49_231430	Putative oligosaccharyl transferase stt3 protein involved in N-linked glycosylation	0.4	12	1	0	0	-3.45	1	2
TGME49_238040	Thioredoxin-like disulfide-isomerase domain-containing protein, Glycosyl transferase family 90	1.19	1	1	0	0	-3.48	1	2
TGME49_314730	ALG6, ALG8 glycosyltransferase family protein, putative enzyme involved in N-linked glycosylation in the ER	1.7	12	1	0	0	-0.97	1	2
TGME49_318730	UDP-N-acetyl-D-galactosamine:polypeptide N-acetylgalactosaminyltransferase-T3	0.57	1	1	0	0	-0.03	1	2
TGME49_259530	GalNac, UDP-N-acetyl-d-galactosamine:polypeptide N-acetylgalactosaminyltransferase T1	0.86	1	1	0	0	1.15	1	2
TGME49_262030	ALG6, ALG8 glycosyltransferase family protein, putative enzyme involved in N-linked glycosylation in the ER	1.21	9	0	0	0	-1.94	1	1
TGME49_255240	Hypothetical protein with non-SMC mitotic condensation complex subunit 1 domain, blastP hit using human PGAP4	0.8	0	0	1	0	-4.28	0	1

Table 8. List of gene candidates scored and ranked for CRISPR targeting of the putative T. gondii GalNAc GPI-transferase. *All values, unless otherwise indicated, were generated by ToxoDB.org at the time of the search: January 2019. (Columns left to right) Gene IDs of Toxoplasma gondii strain ME49 (TGME49) is the most annotated of the 28 strains of T. gondii and, therefore, was the strain used for this text search of gene candidates. Product description provided known and putative characterization of the respective gene I.D. and the 'biological correctness' (i.e. a sugar transferase) basis for in/exclusion of candidates. Nonsynonymous/synonymous SNP ratio is shown. Number of transmembrane domains was preferred to be three, in keeping with the structure of the human PGAP4, but must be a minimum of 1 to meet selection criteria. Expression was binomially scored for 5 FPKM or higher in tachyzoites, the stage that we are using throughout this thesis. EDD was the characterized amino acid sequence of the catalytic domain of human PGAP4 and binomially scored for presence of this motif in the candidate gene. Signal peptides place the protein product in the secretory pathway and/or ER integration which is where GPI synthesis and side chain modifications occur; binomially scored for presence. Mean Phenotype score measured the respective gene contribution to parasite fitness (cultured in HFF) based on a genome-wide CRISPR loss of function screen on GT1 strain background (reference) with negative values indicating the degree to which gene removal adversely impacts parasite survival in HFFs "Biologically correct" category binomially scored the product description such that it was a sugar transferase, but not a product assigned to irrelevant functions (i.e. tRNA synthetase, zinc-finger, GPI backbone synthesis pathway).* *(Continued on p.49)*

(Continued from p. 48) Sum category is the summation of all binomial scores; the resultant total was used to rank the most likely candidates for our target enzyme.

3.7 GalNAc Transferase KO: Gene candidate 259530 on Chromosome VIIb

In our search for the gene responsible for β-GalNAc transferase, our first selected gene was located on chromosome VIIb at position 259530 with the ToxoDB.org product information: GalNAc, UDP-N-acetyl-d-galactosamine : polypeptide N-acetylgalactos-aminyl-transferase (Wojczyk et al., 2003). This promising first target is nestled in chromosome VIIb, in the midst of several SAG-encoding genes, and thus we reasoned this candidate could be the gene by simple 'guilt by association'. Using CRISPR-CAS9, we successfully deleted 259530, creating a RHΔ*ku80*Δ259530 strain, as determined by diagnostic PCR (Figure 11). We expected, if the gene candidate 259530 did encode for the GalNAc transferase enzyme, then staining with two antibodies which detect the two glycoforms of *T. gondii* would be lost, T5-4E10 stains the Gluc-β-GalNAc glycoform, while T3-F12 stains the β-GalNAc glycoform. However, both glycoforms were present in the RHΔ*ku80*Δ259530 with comparable T5-4E10 and T3-F12 staining to the parental RH Δ*ku80*Δ*hxgprt* control (Figure 11C and D).

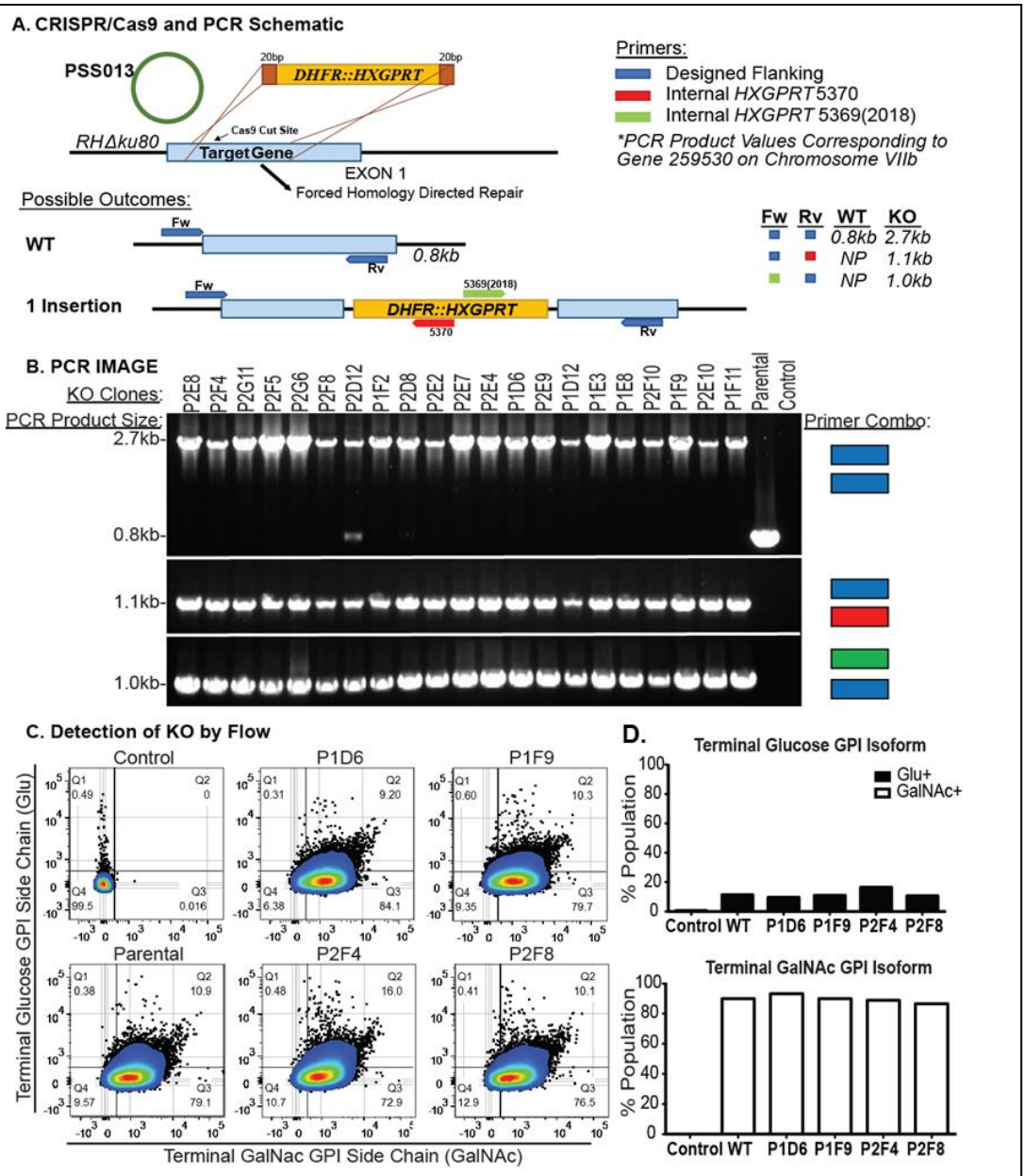

Figure 11. T. gondii GalNAc transferase gene candidate (259530) KO is not the 'droid' we are looking for. A. *CRISPR editing schematic for deleting gene candidate 259530 using Cas9 coded pss013 plasmid, whose guide-RNA targets exon 1 and co-transfected with a drug selectable marker designed to integrate into the Cas9 cut site using the homology directed repair-restricted T. gondii strain RHΔku80. Expected resultant PCR product outcomes are shown.* ***B.*** *PCR confirmation of 259530 KO in all clones.* ***C.*** *Representative flow plots depicting parasite stained for detection of the terminal glucose GPI isoform (Glu+) and terminal GalNAc GPI isoform (GalNAc+). 'Control' flow plot depicts parasite stained with secondary detection antibody only. Frequencies of populations that fall within the gates are indicated. FACS plots generated but not annotated by S. Souza.* ***D.*** *Average frequencies from C of terminal glucose (Glu+) GPI isoform (Q1+Q2) and terminal GalNAc (GalNAc+) GPI isoform (Q2+Q3) expressed by parental or CRISPR edited parasite in one experiment.*

Chapter 4

Discussion

4.1 Protective antibody production against the *T. gondii* GPI anchor: More is better.

From previous unpublished work with a forward genetic screen, *Nfkbid* was implicated as a critical polymorphic genetic determinant responsible for the survival disparity to secondary infection between A/J and B6 mice. Moreover, bumble mice, which lack *Nfkbid* and B-1 cells, were highly susceptible to challenge (unpublished). These observations prompted us to investigate whether there exists a difference in antibody binding of *T. gondii*, generated by resistant and susceptible mice, to the GPI anchor. We show here that following infection in *Nfkbid* null bumble mice, serum IgM and total IgG antibody recognition of parasite antigen is extremely reduced: 87% and 91% total signal loss, respectively, when compared to that of wildtype B6 (Figure 4). Importantly, we saw that A/J and B6 antibody binding profiles to *T. gondii* lysate antigens lower than 50kDa were extremely sensitive to GPI anchor lipid moiety removal. Together, these phenotypes are consistent with the supposition that B-1 antibody responses against the GPI anchor of the SRS surface antigens are important for immunity to *T. gondii*. Mouse antibody clones to the *T. gondii* GPI anchor have been generated (Tomavo et al., 1994) and serum antibody responses to the GPI anchor in humans and rabbits have been observed following infection (Götze et al., 2015; Striepen et al., 1997). Infection with *T. gondii* is known to elicit a robust antibody response to the GPI-attached SRS surface antigens of *T. gondii*. However, our results implicate a large fraction of the antibody repertoire is possibly focused on the GPI anchor, which has not been fully appreciated prior to this dissertation. The exact role of antibody against parasite infection has yet to be pinpointed by our laboratory but, IgM-mediated neutralization (Couper et al., 2005) and IgG-driven opsonization (Joiner et al., 1990) are likely at play.

We further demonstrated that antigen targets of resistant A/J mice are not very (if at all) different from antigen targets of susceptible B6 mice. Subtle differences include inherent propensities of each mouse strain to recognize different epitopes of the P30 antigen (Figure 4, 6, 7), which is likely SAG1. SAG1 is a heavily targeted antigen by antibodies following infection (Tomavo, 1996) and a multi-epitoped antibody response to this antigen may promote better immunity in A/J mice. However, the most notable difference between mouse strains is that A/J mice generate more parasite-specific antibodies on day 5 of challenge compared to B6 (Figure 4, 6, 7). Therefore, our data more strongly supports a

model in which enhanced production parasite-specific antibody during a secondary infection correlates with better protection to virulent *T. gondii* infection.

Interestingly, in all blots we saw no banding pattern below 15kDa which otherwise would have suggested antibody recognition of the GPI anchor independent of protein (Striepen et al., 1997). This lack of signal may simply be due to technical limitations of the SDS-PAGE gel gradient and centrifugation steps of the lysate chosen, which was not designed to enrich for membrane glycolipids. Deletion of the enzyme responsible for the side chain addition to core GPI is an important endeavor as we attempt to demonstrate whether the side chain of *T. gondii* GPI anchors is preferentially targeted by mouse antibodies, which has been shown in humans (Gçtze et al., 2014; Striepen et al., 1997). If side chain recognition is required in mice, then by removing this GPI modification we predict *T. gondii* would evade antibody detection and cause lethal infection in our model. Furthermore, while *T. gondii* does not share the same antigenic variation capabilities as its parasitic brethren, the unique side chain expression may offer a similar result. For example, by upregulating one glycoform over another in response to immune pressures by the host, *T. gondii* may be able to manipulate the host immune response in favor of facilitated immune detection or even alternative immune evasion. This hypothesis is underpinned by the finding that serum IgG antibodies from chronically infected humans and rabbits only recognize the Gluc-β-GalNac but not the β-GalNac GPI glycoform (Gçtze et al., 2014; Striepen et al., 1997). In either case, the identification of the specific antibody binding epitope is critical in the development of completely protective and long-lasting vaccine.

Although it is clear from this study that GPI anchor is a necessary moiety for antigen recognition by protective antibody against *T. gondii*, previous efforts by other labs to generate vaccine using GPI conjugated to a non-toxic diphtheria toxin mutant CRM197 has failed to provide complete protection (Götze et al., 2015). In the *Plasmodium* s.p.p. field, antibody reactivity to purified GPI anchor from *Plasmodium* s.p.p. has been shown to correlate with reduced parasitemia in humans (Naik et al., 2000) and synthetic GPI has been shown to reduce inflammation-associated pathogenesis of cerebral malaria in mice (Schofield et al., 2002). The resolution of the specific side chain contribution to *Plasmodium* immunity is not clear but the contribution of the GPI anchor toward antibody-mediated protection has been underscored. Each of these attempts, however, failed to confer complete protection (survival of virulent live parasite) likely because of their insufficient stimulation of T cell effector responses (Sacks, 2014; Sher, 1992) as a result of parasite protein antigen absence in their vaccine formulations. These crucial findings highlight the need for incorporation of the GPI anchor into vaccine design and novel opportunity to build a better vaccine for the purpose of generating long-lasting immunity against parasite.

Conclusion

The innate and adaptive immune responses are crucial to the control and clearance of parasitic pathogens. As a model organism, *T. gondii* offers a wealth of information to be gleaned in the manipulation of both immune responses. This study offers a small step toward the elucidation of immune detection of *T. gondii*. In the quest for an effective vaccine against parasites, the identification of specific antigen(s) which not only elicits B and T cell response but equally important B-1 cell response as well. We have seen the antibody targets of resistant and susceptible mice are similar, but A/J mice are able to clear secondary infection with the most virulent of *T. gondii* strains. Though this study does not completely resolve the specific epitopes of A/J and B6 antibody, it does offer that A/J antibodies are more highly produced upon secondary infection and this may be key to enhanced immunity to virulent strains. This is suggestively the contribution of the B-1 cell compartment, which may prove the most important cell population to pander to for vaccine development.

References

Albesa-Jove, D., and Guerin, M.E. (2016). The conformational plasticity of glycosyltransferases. Curr. Opin. Struct. Biol. *40*, 23–32.

Alugupalli, K.R., Gerstein, R.M., Chen, J., Szomolanyi-Tsuda, E., Woodland, R.T., and Leong, J.M. (2003). The resolution of relapsing fever borreliosis requires IgM and is concurrent with expansion of B1b lymphocytes. J. Immunol. *170*, 3819–3827.

Alugupalli, K.R., Leong, J.M., Woodland, R.T., Muramatsu, M., Honjo, T., and Gerstein, R.M. (2004). B1b lymphocytes confer T cell-independent long-lasting immunity. Immunity *21*, 379–390.

Arnold, C.N., Pirie, E., Dosenovic, P., McInerney, G.M., Xia, Y., Wang, N., Li, X., Siggs, O.M., Karlsson Hedestam, G.B., and Beutler, B. (2012). A forward genetic screen reveals roles for Nfkbid, Zeb1, and Ruvbl2 in humoral immunity. Proc. Natl. Acad. Sci. *109*, 12286–12293.

Azzouz, N., Shams-eldin, H., Niehus, S., Smith, T.K., and Schwarz, R.T. (2006). Toxoplasma gondii grown in human cells uses GalNAc-containing glycosylphosphatidylinositol precursors to anchor surface antigens while the immunogenic Glc – GalNAc-containing precursors remain free at the parasite cell surface. *38*, 1914–1925.

Bangs, J.D., Doerings, T.L., Englund, P.T., and Hartll, G.W. (1988). Biosynthesis of a Variant Surface Glycoprotein of Trypanosoma brucei. *263*, 17697–17705.

Baumgarth, N. (2011). The double life of a B-1 cell: self-reactivity selects for protective effector functions. Nat. Rev. Immunol. *11*, 34–36.

Baumgarth, N. (2016). B-1 cell heterogeneity and the regulation of natural and antigen-induced IgM production. Front. Immunol. *7*, 1–9.

Baumgarth, N., Herman, O.C., Jager, G.C., Brown, L., Herzenberg, L.A., and Herzenberg, L.A. (1999). Innate and acquired humoral immunities to influenza virus are mediated by distinct arms of the immune system. Proc. Natl. Acad. Sci. U. S. A. *96*, 2250–2255.

Baumgarth, N., Herman, O.C., Jager, G.C., Brown, L.E., Herzenberg, L.A., and Chen, J. (2000a). B-1 and B-2 cell-derived immunoglobulin M antibodies are nonredundant components of the protective response to influenza virus infection. J Exp Med *192*, 271–280.

Baumgarth, N., Chen, J., Herman, O.C., Jager, G.C., and Herzenberg, L.A. (2000b). The role of B-1 and B-2 cells in immune protection from influenza virus infection. Curr. Top. Microbiol. Immunol. *252*, 163–169.

Berland, R., and Wortis, H.H. (2002). ORIGINS AND FUNCTIONS OF B-1 CELLS WITH NOTES ON THE ROLE OF CD5. Annu. Rev. Immunol. *20*, 253–300.

Briles, D.E., Nahm, M., Schroer, K., Davie, J., Baker, P., Kearney, J., and Barletta, R. (1981). Antiphosphocholine antibodies found in normal mouse serum are protective against intravenous infection with type 3 streptococcus pneumoniae. J. Exp. Med. *153*, 694–705.

Brown, C.R., Hunter, C.A., Estes, R.G., Beckmann, E., Forman, J., David, C., Remington, J.S., and McLeod, R. (1995). Definitive identification of a gene that confers resistance against Toxoplasma cyst burden and encephalitis. Immunology *85*, 419–428.

Buzoni-Gatel, D., Lepage, A.C., Dimier-Poisson, I.H., Bout, D.T., and Kasper, L.H. (1997). Adoptive transfer of gut intraepithelial lymphocytes protects against murine infection with Toxoplasma gondii. J. Immunol. *158*, 5883 LP – 5889.

CDC (2017). Toxoplasmosis.

Chakraborty, S., Roy, S., Mistry, H.U., Murthy, S., George, N., Bhandari, V., and Sharma, P. (2017). Potential Sabotage of Host Cell Physiology by Apicomplexan Parasites for Their Survival Benefits. Front. Immunol. *8*, 1261.

Choi, Y.S., and Baumgarth, N. (2008). Dual role for B-1a cells in immunity to influenza virus infection. J. Exp. Med. *205*, 3053–3064.

Chou, M.-Y., Fogelstrand, L., Hartvigsen, K., Hansen, L.F., Woelkers, D., Shaw, P.X., Choi, J., Perkmann, T., Backhed, F., Miller, Y.I., et al. (2009). Oxidation-specific epitopes are dominant targets of innate natural antibodies in mice and humans. J. Clin. Invest. *119*, 1335–1349.

Clayton, L.K., Connolly, J.E., Antonini, V., Keskin, D.B., Osborn, S.L., Kumar, M., Reinherz, E.L., Grusby, M.J., Touma, M., and Bobenchik, A.M. (2007). Functional Role for IkBNS in T Cell Cytokine Regulation As Revealed by Targeted Gene Disruption. J. Immunol. *179*, 1681–1692.

Cole, L.E., Yang, Y., Elkins, K.L., Fernandez, E.T., Qureshi, N., Shlomchik, M.J., Herzenberg, L.A., Herzenberg, L.A., and Vogel, S.N. (2009). Antigen-specific B-1a antibodies induced by Francisella tularensis LPS provide long-term protection against F. tularensis LVS challenge. Proc. Natl. Acad. Sci. U. S. A. *106*, 4343–4348.

Colombo, M.J., and Alugupalli, K.R. (2008). Complement factor H-binding protein, a putative virulence determinant of Borrelia hermsii, is an antigenic target for protective B1b lymphocytes. J. Immunol. *180*, 4858–4864.

Cosenza, H., and Kohler, H. (1972). Specific suppression of the antibody response by antibodies to receptors. Proc. Natl. Acad. Sci. U. S. A. *69*, 2701–2705.

Couper, K.N., Roberts, C.W., Brombacher, F., Alexander, J., and Johnson, L.L. (2005). Toxoplasma gondii-specific immunoglobulin M limits parasite dissemination by preventing host cell invasion. Infect. Immun. *73*, 8060–8068.

Cundill, B., Alexander, N., Bethony, J.M., Diemert, D., Pullan, R.L., and Brooker, S. (2011). Rates and intensity of re-infection with human helminths after treatment and the influence of individual, household, and environmental factors in a Brazilian community. Parasitology *138*, 1406–1416.

Cunningham, A.F., Flores-Langarica, A., Bobat, S., Dominguez Medina, C.C., Cook, C.N.L., Ross, E.A., Lopez-Macias, C., and Henderson, I.R. (2014). B1b cells recognize protective antigens after natural infection and vaccination. Front. Immunol. *5*, 535.

Debierre-Grockiego, F., Campos, M.A., Azzouz, N., Schmidt, J., Bieker, U., Resende, M.G., Mansur, D.S., Weingart, R., Schmidt, R.R., Golenbock, D.T., et al. (2007). Activation of TLR2 and TLR4 by glycosylphosphatidylinositols derived from Toxoplasma gondii. J. Immunol. *179*, 1129–1137.

Eisenhaber, B., Sinha, S., Wong, W.-C., and Eisenhaber, F. (2018). Function of a membrane-embedded domain evolutionarily multiplied in the GPI lipid anchor pathway proteins PIG-B, PIG-M, PIG-U, PIG-W, PIG-V, and PIG-Z. Cell Cycle *17*, 874–880.

Elbez-Rubinstein, A., Ajzenberg, D., Dardé, M., Cohen, R., Dumètre, A., Yera, H., Gondon, E., Janaud, J., and Thulliez, P. (2009). Congenital Toxoplasmosis and Reinfection during Pregnancy: Case Report, Strain Characterization, Experimental Model of Reinfection, and Review. J. Infect. Dis. *199*, 280–285.

Englund, P.T. (1993). THE STRUCTURE AND BIOSYNTHESIS OF GLYCOSYL PHOSPHATIDYLINOSITOL PROTEIN ANCHORS. Annu. Rev. Biochem. *62*, 121–138.

Ferguson, M. A., Low, M. G., and Cross, G.A. (1985). Glycosylsn-1,2-dimyristylphosphatidylinositol is covalently linked to Trypanosoma brucei variant surface glycoprotein. J. Biol. Chem. *260*, 14547–14555.

Ferguson, M.A. (1999). The structure, biosynthesis and functions of glycosylphosphatidylinositol anchors, and the contributions of trypanosome research. J. Cell Sci. *112*, 2799–2809.

Ferguson, M.A., Homans, S.W., Dwek, R.A., and Rademacher, T.W. (1988). Glycosyl-phosphatidylinositol moiety that anchors Trypanosoma brucei variant surface glycoprotein to the membrane. Science (80-.). *239*, 753–759.

Fontaine, T., Magnin, T., Melhert, A., Lamont, D., Latgé, J.P., and Ferguson, M.A.J. (2003). Structures of the glycosylphosphatidylinositol membrane anchors from Aspergillus fumigatus membrane proteins. Glycobiology *13*, 169–177.

Gay, G., Braun, L., Brenier-Pinchart, M.-P., Vollaire, J., Josserand, V., Bertini, R.-L., Varesano, A., Touquet, B., De Bock, P.-J., Coute, Y., et al. (2016). Toxoplasma gondii TgIST co-opts host chromatin repressors dampening STAT1-dependent gene regulation and IFN-γ-mediated host defenses. J. Exp. Med. *213*, 1779–1798.

Gazzinelli, R.T., Hakim, F.T., Hieny, S., Shearer, G.M., and Sher, A. (1991). Synergistic role of CD4+ and CD8+ T lymphocytes in IFN-gamma production and protective

immunity induced by an attenuated Toxoplasma gondii vaccine. J. Immunol. *146*, 286 LP – 292.

Gçtze, S., Azzouz, N., Tsai, Y.-H., Groß, U., Reinhardt, A., Anish, C., Seeberger, P.H., and Silva, D.V. (2014). Diagnosis of Toxoplasmosis Using a Synthetic Glycosylphosphatidylinositol Glycan. Angew. Chemie Int. Ed. *53*, 13701–13705.

Gigley, J.P., Fox, B.A., and Bzik, D.J. (2009). Cell-Mediated Immunity to Toxoplasma gondii Develops Primarily by Local Th1 Host Immune Responses in the Absence of Parasite Replication. J. Immunol. *182*, 1069 LP – 1078.

Gigley, J.P., Bhadra, R., and Khan, I.A. (2011). CD8 T Cells and Toxoplasma gondii: A New Paradigm. J. Parasitol. Res. *2011*, 243796.

Gil-Cruz, C., Bobat, S., Marshall, J.L., Kingsley, R.A., Ross, E.A., Henderson, I.R., Leyton, D.L., Coughlan, R.E., Khan, M., Jensen, K.T., et al. (2009). The porin OmpD from nontyphoidal Salmonella is a key target for a protective B1b cell antibody response. Proc. Natl. Acad. Sci. U. S. A. *106*, 9803–9808.

Götze, S., Reinhardt, A., Geissner, A., Azzouz, N., Tsai, Y.H., Kurucz, R., Silva, D.V., and Seeberger, P.H. (2015). Investigation of the protective properties of glycosylphosphatidylinositol-based vaccine candidates in a Toxoplasma gondii mouse challenge model. Glycobiology *25*, 984–991.

Greenberg, S.G., Davies, P., Schein, J.D., and Binder, L.I. (1992). Hydrofluoric acid-treated tau PHF proteins display the same biochemical properties as normal tau. J. Biol. Chem. *267*, 564–569.

Guérardel, Y., Niehus, S., Debierre-Grockiego, F., Coddeville, B., Elass, E., and Schwarz, R.T. (2011). Glycosylphosphatidylinositols of Toxoplasma gondii induce matrix metalloproteinase-9 production and degradation of galectin-3. Immunobiology *217*, 61–64.

Haas, K.M., Poe, J.C., Steeber, D.A., and Tedder, T.F. (2005). B-1a and B-1b cells exhibit distinct developmental requirements and have unique functional roles in innate and adaptive immunity to S. pneumoniae. Immunity *23*, 7–18.

Hassan, M.A.., Butty, V.., Jensen, K.D.., and Saeij, J.P. (2014). The genetic basis for individual differences in mRNA splicing and APOBEC1 editing activity in murine macrophages. Genome Res. *24*, 377–389.

Hassan, M.A.., Jensen, K.D.., Butty, V.., Hu, K.., Boedec, E.., Prins, P.., and Saeij, J.P. (2015). Transcriptional and Linkage Analyses Identify Loci that Mediate the Differential Macrophage Response to Inflammatory Stimuli and Infection. PLoS Genet. *11*, e1005619.

Hayakawa, K., Asano, M., Shinton, S.A., Gui, M., Allman, D., Stewart, C.L., Silver, J., and Hardy, R.R. (1999). Positive selection of natural autoreactive B cells. Science *285*, 113–116.

Hirata, T., Mishra, S.K., Nakamura, S., Saito, K., Motooka, D., Takada, Y., Kanzawa, N., Murakami, Y., Maeda, Y., Fujita, M., et al. (2018). Identification of a Golgi GPI-N-acetylgalactosamine transferase with tandem transmembrane regions in the catalytic domain. Nat. Commun. *9*, 405.

Hirotani, T., Lee, P.Y., Kuwata, H., Yamamoto, M., Matsumoto, M., Kawase, I., Akira, S., and Takeda, K. (2005). The nuclear IκB protein IκBNS selectively inhibits lipopolysaccharide-induced IL-6 production in macrophages of the colonic lamina propria. J. Immunol. *174*, 3650–3657.

Hirotani, T., Takeda, K., Matsumoto, M., Morishita, H., Atarashi, K., Kuwata, H., and Koga, R. (2006). IκBNS Inhibits Induction of a Subset of Toll-like Receptor-Dependent Genes and Limits Inflammation. Immunity *24*, 41–51.

Homans, S.W., Ferguson, M.A., Dwek, R.A., Rademacher, T.W., Anand, R., and Williams, A.F. (1988). Complete structure of the glycosyl phosphatidylinositol membrane anchor of rat brain Thy-1 glycoprotein. Nature *333*, 269–272.

Hoseinian Khosroshahi, K., Ghaffarifar, F., D'Souza, S., Sharifi, Z., and Dalimi, A. (2011). Evaluation of the immune response induced by DNA vaccine cocktail expressing complete SAG1 and ROP2 genes against toxoplasmosis. Vaccine *29*, 778–783.

Hotez, P.J., Alvarado, M., Basáñez, M.-G., Bolliger, I., Bourne, R., Boussinesq, M., Brooker, S.J., Brown, A.S., Buckle, G., Budke, C.M., et al. (2014). The Global Burden of Disease Study 2010: Interpretation and Implications for the Neglected Tropical Diseases. PLoS Negl. Trop. Dis. *8*, e2865.

Howard, J.C.., Hunn, J.P.., and Steinfeldt, T. (2011). The IRG protein-based resistance mechanism in mice and its relation to virulence in Toxoplasma gondii. Curr. Opin. Microbiol. *14*, 414–421.

Ismael, A.B., Sekkai, D., Collin, C., Bout, D., and Mevelec, M.N. (2003). The MIC3 gene of Toxoplasma gondii is a novel potent vaccine candidate against toxoplasmosis. Infect. Immun. *71*, 6222–6228.

Jacot, D., Meissner, M., Sheiner, L., Soldati-Favre, D., and Striepen, B. (2013). Genetic Manipulation of Toxoplasma gondii.

Jensen, K.D.C., Camejo, A., Melo, M.B., Cordeiro, C., Julien, L., Grotenbreg, G.M., Frickel, E.M., Ploegh, H.L., Young, L., and Saeij, J.P.J. (2015). Toxoplasma gondii superinfection and virulence during secondary infection correlate with the exact ROP5/ROP18 allelic combination. MBio *6*, 1–15.

Joiner, K.A., Fuhrman, S.A., Miettinen, H.M., Kasper, L.H., and Mellman, I. (1990). Toxoplasma gondii: fusion competence of parasitophorous vacuoles in Fc receptor-transfected fibroblasts. Science *249*, 641–646.

Jordan, K.A., Wilson, E.H., Tait, E.D., Fox, B.A., Roos, D.S., Bzik, D.J., Dzierszinski, F., and Hunter, C.A. (2009). Kinetics and phenotype of vaccine-induced CD8+ T-cell responses to Toxoplasma gondii. Infect. Immun. *77*, 3894–3901.

Khan, I.A., Schwartzman, J.D., Matsuura, T., and Kasper, L.H. (1997). A dichotomous role for nitric oxide during acute Toxoplasma gondii infection in mice. Proc. Natl. Acad. Sci. U. S. A. *94*, 13955–13960.

Kieffer, F., and Wallon, M. (2013). Congenital toxoplasmosis. Handb. Clin. Neurol. *112*, 1099–1101.

Kulik, L., Fleming, S.D., Moratz, C., Reuter, J.W., Novikov, A., Chen, K., Andrews, K.A., Markaryan, A., Quigg, R.J., Silverman, G.J., et al. (2009). Pathogenic natural antibodies recognizing annexin IV are required to develop intestinal ischemia-reperfusion injury. J. Immunol. *182*, 5363–5373.

Labun, K., Montague, T.G., Gagnon, J.A., Thyme, S.B., and Valen, E. (2016). CHOPCHOP v2: a web tool for the next generation of CRISPR genome engineering. Nucleic Acids Res. *44*, W272–W276.

Lindsay, D.S., and Dubey, J.P. (2011). Toxoplasma gondii: the changing paradigm of congenital toxoplasmosis. J. Parasitol. *9*, 1–3.

Low, M., Hoessli, D. C., and Ilangumaran, S., E. (1999). GPI-anchored biomolecules an overview. In GPI-Anchored Membrane Proteins and Carbohydrates, (Austin, TX: Landes Company), pp. 1–14.

Low, M.G. (1987). Biochemistry of the glycosyl-phosphatidylinositol membrane protein anchors. Biochem. J. *244*, 1–13.

Luft, B.J.., Hafner, R., Korzun, A.H.., Leport, C., Antoniskis, D., Bosler, E.M.., Bourland, D. David; Uttamchandani, R., Fuhrer, J., Jacobson, J., Morlat, P., et al. (1993). Toxoplasmic Encephalitis in Patients with the Acquired Immunodeficiency Syndrome. N. Engl. J. Med. *329*, 995–100.

Manger, I.D., Hehl, A.B., and Boothroyd, J.C. (1998). The surface of Toxoplasma tachyzoites is dominated by a family of glycosylphosphatidylinositol-anchored antigens related to SAG1. Infect. Immun. *66*, 2237–2244.

Mayor, S., Menon, A.K., Cross, G.A.M., Ferguson, M.A.J., Dwek, R.A., and Rademacher, T.W. (1990a). Glycolipid precursors for the membrane anchor of Trypanosoma brucei variant surface glycoproteins. J.Biol.Chem. *265*, I.

Mayor, S., Menon, A.K., Cross, G.A.M., Ferguson, M.A.J., Dwek, R.A., and Rademacher, T.W. (1990b). Glycolipid precursors for the membrane anchor of Trypanosoma brucei variant surface glycoproteins. J.Biol.Chem. *265*, I.

McAuley, J. (1994). Early and Longitudinal Evaluations of Treated Infants and Children and Untreated Historical Patients With Congenital Toxoplasmosis. Pediatr. Infect. Dis. J. *13*, 844.

McLeod, R.., Skamene, E.., Brown, C.R.., Eisenhauer, P.B.., and Mack, D.G. (1989). Genetic regulation of early survival and cyst number after peroral Toxoplasma gondii infection of A x B/B x A recombinant inbred and B10 congenic mice. J. Immunol. *143*,

3031–3034.

Menon, A.K., Mayor, S., and Schwarz, R.T. (1990). Biosynthesis of glycosyl-phosphatidylinositol lipids in Trypanosoma brucei: involvement of mannosyl-phosphoryldolichol as the mannose donor. EMBO J. *9*, 4249–4258.

Menon, A.K., Eppingerl, M., Mayor, S., and Schwarz, R.T. (1993). Phosphatidylethanolamine is the donor of the terminal phosphoethanolamine group in trypanosome glycosyl- IUDP-G1cNACI. *1*.

Miura, M., Hasegawa, N., Noguchi, M., Sugimoto, K., and Touma, M. (2016). The atypical IκB protein IκB(NS) is important for Toll-like receptor-induced interleukin-10 production in B cells. Immunology *147*, 453–463.

Montague, T.G., Cruz, J.M., Gagnon, J.A., Church, G.M., and Valen, E. (2014). CHOPCHOP: a CRISPR/Cas9 and TALEN web tool for genome editing. Nucleic Acids Res. *42*, W401-7.

Nagasawa, H., Maekawa, Y., Himeno, K., Oka, M., and Manabe, T. (2013). Role of L3T4 + and Lyt-2 + T Cell Subsets in Protective Immune Responses of Mice against Infection with a Low or High Virulent Strain of Toxoplasma gondii . Microbiol. Immunol. *35*, 215–222.

Nagel, S.D., and Boothroyd, J.C. (1989). The major surface antigen, P30, of Toxoplasma gondii is anchored by a glycolipid. J. Biol. Chem. *264*, 5569–5574.

Naik, R.S., Branch, O.H., Woods, A.S., Vijaykumar, M., Perkins, D.J., Nahlen, B.L., Lal, A.A., Cotter, R.J., Costello, C.E., Ockenhouse, C.F., et al. (2000). Glycosylphosphatidylinositol anchors of Plasmodium falciparum: molecular characterization and naturally elicited antibody response that may provide immunity to malaria pathogenesis. J. Exp. Med. *192*, 1563–1576.

Niedelman, W., Gold, D.A., Rosowski, E.E., Sprokholt, J.K., Lim, D., Farid Arenas, A., Melo, M.B., Spooner, E., Yaffe, M.B., and Saeij, J.P.J. (2012). The rhoptry proteins ROP18 and ROP5 mediate Toxoplasma gondii evasion of the murine, but not the human, interferon-gamma response. PLoS Pathog. *8*, e1002784–e1002784.

Nosjean, O., Briolay, A., and Roux, B. (1997). Mammalian GPI proteins: sorting, membrane residence and functions. Biochim Biophys Acta *1331*, 153–186.

Olias, P., Etheridge, R.D., Zhang, Y., Holtzman, M.J., and Sibley, L.D. (2016). Toxoplasma Effector Recruits the Mi-2/NuRD Complex to Repress STAT1 Transcription and Block IFN-γ-Dependent Gene Expression. Cell Host Microbe *20*, 72–82.

Paulick, M.G., and Bertozzi, C.R. (2008). The Glycosylphosphatidylinositol Anchor : A Complex Membrane-Anchoring. Biochemistry *47*, 6991–7000.

Pedersen, G.K., Ádori, M., Stark, J.M., Khoenkhoen, S., Arnold, C., Beutler, B., and Karlsson Hedestam, G.B. (2016). Heterozygous Mutation in IκBNS Leads to Reduced Levels of Natural IgM Antibodies and Impaired Responses to T-Independent Type 2

Antigens. Front. Immunol. *7*, 65.

Pinzan, C.F., Sardinha-Silva, A., Almeida, F., Lai, L., Lopes, C.D., Lourenço, E.V., Panunto-Castelo, A., Matthews, S., and Roque-Barreira, M.C. (2015). Vaccination with Recombinant Microneme Proteins Confers Protection against Experimental Toxoplasmosis in Mice. PLoS One *10*, e0143087.

Pullan, R.L., Smith, J.L., Jasrasaria, R., and Brooker, S.J. (2014). Global numbers of infection and disease burden of soil transmitted helminth infections in 2010. Parasit. Vectors *7*, 37.

RTS Clincal Trials Partnership (2015). Efficacy and safety of RTS,S/AS01 malaria vaccine with or without a booster dose in infants and children in Africa: final results of a phase 3, individually randomised, controlled trial. Lancet (London, England) *386*, 31–45.

Sacks, D.L. (2014). Vaccines against tropical parasitic diseases: A persisting answer to a persisting problem. Nat. Immunol. *15*, 403–405.

Schofield, L., Hewitt, M.C., Evans, K., Siomos, M.-A., and Seeberger, P.H. (2002). Synthetic GPI as a candidate anti-toxic vaccine in a model of malaria. Nature *418*, 785–789.

Schuster, M., Glauben, R., Plaza-Sirvent, C., Schreiber, L., Annemann, M., Floess, S., Kühl, A.A., Clayton, L.K., Sparwasser, T., Schulze-Osthoff, K., et al. (2012). IκBNS Protein Mediates Regulatory T Cell Development via Induction of the Foxp3 Transcription Factor. Immunity *37*, 998–1008.

Schuster, M., Annemann, M., Plaza-Sirvent, C., and Schmitz, I. (2013). Atypical IkappaB proteins - nuclear modulators of NF-kappaB signaling. Cell Commun Signal *11*, 23.

Seeberger, P.H., Azzouz, N., Varon Silva, D., Götze, S., Hahm, H.S., and Tsai, Y.-H. (2011). A General Method for Synthesis of GPI Anchors Illustrated by the Total Synthesis of the Low-Molecular-Weight Antigen from Toxoplasma gondii. Angew. Chemie Int. Ed. *50*, 9961–9964.

Sher, A. (1992). REGULATION OF IMMUNITY TO PARASITES BY T CELLS AND T CELL-DERIVED CYTOKINES. Annu. Rev. Immunol. *10*, 385–409.

Shirahata, T., Yamashita, T., Ohta, C., Goto, H., and Nakane, A. (1994). CD8+ T Lymphocytes Are the Major Cell Population Involved in the Early Gamma Interferon Response and Resistance to Acute Primary Toxoplasma gondii Infection in Mice. Microbiol. Immunol. *38*, 789–796.

Smith, F.L., and Baumgarth, N. (2019). B-1 cell responses to infections. Curr. Opin. Immunol. *57*, 23–31.

Smith, T.K., Azzouz, N., Gerold, P., Seeber, F., Lingelbach, K., and Schwarz, R.T. (2006). Membrane Topology and Transient Acylation of Toxoplasma gondii Glycosylphosphatidylinositols. Eukaryot. Cell *5*, 1420–1429.

Smith, T.K., Azzouz, N., Shams-eldin, H., and Schwarz, R.T. (2007). The Role of

Inositol Acylation and Inositol Deacylation in the Toxoplasma gondii Glycosylphosphatidylinositol Biosynthetic Pathway. J. Biol. Chem. *282*, 32032–32042.

Splitt, S.D., Souza, S.P., Valentine, K.M., Castellanos, B.E., Curd, A.B., Hoyer, K.K., and Jensen, K.D.C. (2018). PD-L1, TIM-3, and CTLA-4 Blockade Fails To Promote Resistance to Secondary Infection with Virulent Strains of Toxoplasma gondii. Infect. Immun. *86*, e00459-18.

Striepen, B., Tomavo, S., Dubremetz, J.F., and Schwarz, R.T. (1992). Identification and characterisation of glycosyl-inositolphospholipids in Toxoplasma gondii. Biochem. Soc. Trans. *20*, 296S.

Striepen, B., Zinecker, C.F., Damm, J.B.L., Melgers, P.A.T., Gerwig, G.J., Koolen, M., Vliegenthart, J.F.G., Dubremetz, J.F., and Schwarz, R.T. (1997). Molecular structure of the "low molecular weight antigen" of Toxoplasma gondii: A glucose α1-4 N-acetylgalactosamine makes free glycosyl-phosphatidylinositols highly immunogenic. J. Mol. Biol. *266*, 797–813.

Suzuki, Y., and Remington, J.S. (1988). Dual regulation of resistance against Toxoplasma gondii infection by Lyt-2+ and Lyt-1+, L3T4+ T cells in mice. J. Immunol. *140*, 3943 LP – 3946.

Suzuki, Y., and Remington, J.S. (1990). The effect of anti-IFN-gamma antibody on the protective effect of Lyt-2+ immune T cells against toxoplasmosis in mice. J. Immunol. *144*, 1954 LP – 1956.

Swisher, C.N., Boyer, K., and McLeod, R. (1994). Congenital toxoplasmosis. The Toxoplasmosis Study Group. Semin Pediatr Neurol *1*, 4–25.

Tomavo, S. (1996). The major surface proteins of Toxoplasma gondii: structures and functions. Curr. Top. Microbiol. Immunol. *219*, 45–54.

Tomavo, S., Schwarz, R.T., and Dubremetz, J.F. (1989). Evidence for glycosyl-phosphatidylinositol anchoring of Toxoplasma gondii major surface antigens. Mol. Cell. Biol. *9*, 4576–4580.

Tomavo, S., Dubremetz, J.F., and Schwarz, R.T. (1992a). Cell-free synthesis of glycolipid candidate precursor(s) for glycosyl-phosphatidylinositol anchors of Toxoplasma gondii surface proteins. Biochem. Soc. Trans. *20*, 166S.

Tomavo, S., Dubremetz, J.F., and Schwarz, R.T. (1992b). Biosynthesis of glycolipid precursors for glycosylphosphatidylinositol membrane anchors in a Toxoplasma gondii cell-free system. J. Biol. Chem. *267*, 21446–21458.

Tomavo, S., Dubremetz, J.F., and Schwarz, R.T. (1992c). A family of glycolipids from Toxoplasma gondii. Identification of candidate glycolipid precursor(s) for Toxoplasma gondii glycosylphosphatidylinositol membrane anchors. J. Biol. Chem. *267*, 11721–11728.

Tomavo, S., Martinage, A., and Dubremetz, J.F. (1992d). Phosphorylation of

Toxoplasma gondii major surface antigens. Parasitol. Res. *78*, 541–544.

Tomavo, S., Couvreur, G., Leriche, M.A., Sadak, A., Achbarou, A., Fortier, B., and Dubremetz, J.F. (1994). Immunolocalization and characterization of the low molecular weight antigen (4-5 kDa) of Toxoplasma gondii that elicits an early IgM response upon primary infection. Parasitology *108 (Pt 2*, 139–145.

Torgerson, P.R., de Silva, N.R., Fevre, E.M., Kasuga, F., Rokni, M.B., Zhou, X.-N., Sripa, B., Gargouri, N., Willingham, A.L., and Stein, C. (2014). The global burden of foodborne parasitic diseases: an update. Trends Parasitol. *30*, 20–26.

Torgerson, P.R., Devleesschauwer, B., Praet, N., Speybroeck, N., Willingham, A.L., Kasuga, F., Rokni, M.B., Zhou, X.N., Fèvre, E.M., Sripa, B., et al. (2015). World Health Organization Estimates of the Global and Regional Disease Burden of 11 Foodborne Parasitic Diseases, 2010: A Data Synthesis. PLoS Med. *12*, 1–22.

Touma, M., Keskin, D.B., Shiroki, F., Saito, I., Koyasu, S., Reinherz, E.L., and Clayton, L.K. (2011). Impaired B Cell Development and Function in the Absence of IκBNS. J. Immunol. *187*, 3942–3952.

Wiggins, C.A., and Munro, S. (1998). Activity of the yeast MNN1 alpha-1,3-mannosyltransferase requires a motif conserved in many other families of glycosyltransferases. Proc. Natl. Acad. Sci. U. S. A. *95*, 7945–7950.

Wojczyk, B.S., Stwora-Wojczyk, M.M., Hagen, F.K., Striepen, B., Hang, H.C., Bertozzi, C.R., Roos, D.S., and Spitalnik, S.L. (2003). cDNA cloning and expression of UDP-N-acetyl-d-galactosamine:polypeptide N-acetylgalactosaminyltransferase T1 from Toxoplasma gondii. Mol. Biochem. Parasitol. *131*, 93–107.

Y Suzuki, MA Orellana, RD Schreiber, J.R. (1988). Interferon-gamma: the major mediator of resistance against Toxoplasma gondii. Science (80-.). *240*, 516–518.

Y Suzuki, F.K.C. and J.S.R. (1989). Importance of endogenous IFN-gamma for prevention of toxoplasmic encephalitis in mice. J. Immunol. *143*, 2045–2050.

Yang, Y., Ghosn, E.E.B., Cole, L.E., Obukhanych, T. V, Sadate-Ngatchou, P., Vogel, S.N., Herzenberg, L.A., and Herzenberg, L.A. (2012). Antigen-specific antibody responses in B-1a and their relationship to natural immunity. Proc. Natl. Acad. Sci. U. S. A. *109*, 5382–5387.

Yarovinsky, F. (2014). Innate immunity to Toxoplasma gondii infection. Nat. Rev. Immunol. *14*, 109.

Zinecker, C.F., Striepen, B., Geyer, H., Geyer, R., Dubremetz, J.F., and Schwarz, R.T. (2001). Two glycoforms are present in the GPI-membrane anchor of the surface antigen 1 (P30) of Toxoplasma gondii. Mol. Biochem. Parasitol. *116*, 127–135.